

**Quantifying the legacy of coal combustion products in riverine sediments**

by

Emma Dawn Henderson

A thesis submitted to the Graduate Faculty of  
Auburn University  
in partial fulfillment of the  
requirements for the Degree of  
Geology, Master of Science

Auburn, Alabama  
May 4, 2024

Keywords: Spheroidal carbonaceous particles; coal fly ash; metal enrichment

Copyright 2024 by Emma Dawn Henderson

Approved by

Dr. Ann S. Ojeda, Co-Chair, Assistant Professor, Geoscience  
Dr. Richard S. Vachula, Co-Chair, Assistant Professor, Geoscience  
Dr. Ming-Kuo Lee, Chair, Geosciences

## Abstract

Coal fired power plants (CFPPs) produce much of the world's energy and generate large quantities of coal combustion products (CCPs), including organic material (OM), fly ash, bottom ash, spheroidal carbonaceous particles (SCPs) and metals, much of which is stored near CFPPs. Despite projected closures of CFPPs, these waste products will persist and can potentially impact environments. Here, we develop a new method for SCP enumeration by analyzing 14 riverine sediment sites and then use bootstrapping techniques to quantify measurement precision as a function of subsample number. We recommend the enumeration of SCPs in sets of at least 10 subsamples per site to maximize precision and minimize error. Next, using SCP, toxic metal, and OM concentrations, we explore the differences in CFPP contamination near an active and a legacy (closed) plant. We find that for our study sites, SCPs are a better proxy for CCP environmental impacts than toxic metal or OM concentrations. SCP concentrations are highest near the active CFPP but also are present near the legacy CFPP. Even after coal combustion ceases and impoundments are closed, CCPs persist in the environment.

## Acknowledgments

First, I would like to thank my co-advisors, beginning with Dr. Ann Ojeda. Working with her first as an undergraduate researcher and now as a graduate student has shaped my perspective on what it means to conduct good science. I am thankful for the opportunities I have had learning with her.

I would like to thank my co-advisor Dr. Richard Vachula for joining this journey with me, and for guiding and supporting me these past two years. I feel that I have gained confidence in myself as a scientist, presenter, and author in working with him. I am thankful for the lessons I have learned and for the experience gained in working with him.

I would like to thank my committee member, Dr. Ming-Kuo Lee, for his support and guidance throughout my time here at Auburn, both as an undergraduate and a graduate student.

Secondly, I would like to thank the Ojeda and Vachula lab groups for their feedback, questions, and friendship. I consider working with each of you to be one of the highlights of my time as a graduate student here at Auburn. To Sidney, thank you for being an excellent friend, field partner, and office mate, and for letting me join you on all your adventures. I know you will do great things wherever life takes you next. To Dr. Natalia Malina, thank you for always answering my questions above and beyond what I had asked, for your willingness to teach, and for your patience when I still didn't know what was going on.

I couldn't write an acknowledgements section, without mentioning the Department of Geosciences. The friendship and community I found here were crucial to the success I had as a graduate student. I enjoyed being a part of this department because of each and every one of you.

Thirdly, I would like to thank my family and friends for their love and support. To my sister Lydia, thank you for being my best friend and for your feedback on the hundreds of figures, emails, and projects I've sent you over the years. To my parents, thank you for instilling in me a love for science and the environment. Thank you for believing in me and giving me the tools I needed for success. Kerstin, thank you for the much-needed breaks to Nevada throughout my graduate program, and for your friendship. To my book club, thank you for the laughs and giving me a reason to take breaks to read. To Mopsy and Tippy, you both are an inspiration and truly a muse for all that I do. Lastly, I would like to thank God for being a source of eternal peace in what has been probably the most stressful period of my life.

I dedicate this thesis to my younger self, who was always eager to learn, curious about the world, and who looked for cool rocks to carry home. May I never forget her.

War Eagle!

## Table of Contents

Abstract .....	2
Acknowledgments.....	3
List of Tables .....	6
List of Figures .....	7
List of Abbreviations .....	8
Chapter 1: Introduction.....	9
Chapter 2: Is once enough? The effect of subsampling on spheroidal carbonaceous particle (SCP) quantification .....	11
2.1 Abstract.....	11
2.2 Introduction.....	12
2.3 Materials and Procedures .....	15
2.3.1 SCP quantification .....	15
2.3.2 Bootstrapping.....	16
2.4 Assessment.....	18
2.5 Discussion.....	23
2.5.1 Quantifying SCPs with subsampling .....	23
2.5.2 SCPs and the Anthropocene.....	25
2.6 Comments and recommendations .....	28

Chapter 3: Comparing sedimentary impacts of coal combustion from active and inactive coal fired power plants .....	29
3.1 Abstract .....	29
3.2 Introduction.....	31
3.3 Materials and methods .....	36
3.3.1 Study sites .....	36
3.3.2 Sediment collection and analysis .....	37
3.3.3 Statistics .....	38
3.4 Results and discussion .....	40
3.4.1 Relationships between SCPs, toxic metals, and OM .....	40
3.4.2 Metal enrichment factors compared to other CCP-impacted sites.....	43
3.5 Environmental implications .....	46
Chapter 4: Summary and Outlook .....	49
References.....	51
Appendix 1: Chapter 2 Supplementary information.....	68
Appendix 2: Chapter 3 Supplementary information.....	86

## List of Tables

Table 2.1 Summary statistics for raw and bootstrapped SCP concentration data.....	17
Table S.2.1 Site information for Figure 2.5 .....	65
Table S.3.1 Percent weight of OM and bootstrapped SCP.....	82
Table S.3.2 Raw sediment metal concentrations .....	83

## List of Figures

Figure 2.1 Conceptual diagram of the bootstrapping workflow .....	14
Figure 2.2 The bootstrapped means and RSDs for each sample.....	18
Figure 2.3 Raw SCP sample means, percent probability of zero SCPs, and RSDs.....	19
Figure 2.4 Bootstrapped upper and lower 95% confidence intervals for samples with <10 SCPs/gDM .....	20
Figure 2.5 Global sites of SCP enumeration.....	24
Figure 3.1 U.S. coal combustion product impoundments .....	32
Figure 3.2 Study site map .....	35
Figure 3.3 Metal and SCP concentrations near the active and legacy CFPPs .....	40
Figure 3.4 Sediment metal enrichment factors .....	43
Figure S.3.1 SCP enumeration strategy diagram.....	84

## List of Abbreviations

SCP	Spheroidal Carbonaceous Particle
gDM	gram of Dry Mass sediment
SD	Standard Deviation
RSD	Relative Standard Deviation
CFPP	Coal Fired Power Plant
CCP	Coal Combustion Product
PAH	Polycyclic Aromatic Hydrocarbon
EPA	Environmental Protection Agency
US(A)	United States (of America)
AL	Alabama
MS	Mississippi
TN	Tennessee
GA	Georgia
FL	Florida

## Chapter 1: Introduction

Coal combustion is a dominant global source of energy (EIA, 2023). Coal combustion products (CCPs) encompass a variety of materials including surface runoff, leachates, fly ash, bottom ash, and slag (Deonarine et al., 2023; Wang et al., 2022). Traditionally, sediment metal enrichment has been used as a proxy for detecting impacts from coal fired power plants (CFPPs) (Ramsey et al., 2019; Ruhl et al., 2010; Vengosh et al., 2019; Wang et al., 2022). Novel studies include additional proxies such as sediment magnetic susceptibility or the visual identification of fly ash particles to further prove the presence of CCPs in the environment (Cowan et al., 2017; Wang et al., 2022). Spheroidal carbonaceous particles (SCPs), a unique byproduct of coal combustion, have long been used as a proxy for CFPPs within the sediment record (Boyle et al., 1998; Broman et al., 1990; Inoue et al., 2022; Rose, 2008; Rose et al., 2012; Swindles, 2010). SCPs are an ideal CFPP proxy as they are easily identifiable in sediments and remain relatively recalcitrant after deposition (Rose, 2008).

Although the field of SCP studies has grown and developed, the method quantifying them in sediments has not. The traditional method for SCP enumeration assumes a single quantification of SCPs is representative of the true concentration for a sample or section of a core. In reality, identifying the concentration and spatial distribution of SCPs in the environment requires precise, standardized, and reliable quantification methods. Previous analyses of enumeration methodologies similar to that of SCPs have consistently found that single subsamples provide an imperfect picture of overall sedimentary concentrations (Anderson et al., 2022; Comtois et al., 1999; Doberstein et al., 2000; Kemp et al., 2020; Schlachter & Horn, 2010).

The overarching questions driving this thesis research were:

1. How does SCP measurement uncertainty affect total site measurement error?
2. What are the differences in environmental contamination between active and closed coal fired power plants?

In Chapter 2, we propose a new method for SCP quantification that is more robust than and provides statistical advantages over the traditional enumeration method. Not only does Chapter 2 propose a new method, but this study is also the first of its kind to employ SCP enumeration in riverine sediments, and not in basinal settings like lakes, peats, or other reservoirs. In Chapter 3, we use the new SCP enumeration method to explore the relationships between SCP, trace metal, and organic matter (OM) concentrations between sediments near an active and near a legacy (closed) CFPP, which is now also a legacy site of CCP storage. Chapter 4 summarizes the work of Chapters 2 and 3 and provides an outlook on future directions of this research.

## **Chapter 2: Is once enough? The effect of subsampling on spheroidal carbonaceous particle (SCP) quantification**

Authors: Emma D. Henderson, Ann S. Ojeda, and Richard S. Vachula

This chapter was submitted for publication to *Limnology and Oceanography: Methods* on 21 February 2024.

### **2.1 Abstract**

Spheroidal carbonaceous particles (SCPs) are preserved in lacustrine, estuarine, and riverine sediments and can indicate anthropogenic pollution or provide chronology for cores. SCPs are only produced during the combustion of fossil fuels, with fluctuations in SCP concentrations typically corresponding to changes in fossil fuel combustion. While the usage of SCPs as indicators is increasing, the enumerative method of quantifying their sedimentary concentrations has remained virtually unchanged, and assumes that one subsample is representative of total site abundance. We present a new method of SCP quantification employing the enumeration of multiple subsamples, increasing the precision and accuracy of SCP concentration measurements. We quantified SCPs in sets of 30 subsamples for 14 riverine sites (n=420). SCP concentrations varied (0 SCPs/gDM - 2141 SCPs/gDM), reflecting the typical range of SCP concentrations in other environmental settings. For each site, we used a bootstrapping method to approximate the theoretical mean of SCPs at 1-30 subsample sizes then compared the theoretical mean and relative standard deviation. We found that enumerating 10 subsamples per site better represents the theoretical mean of SCPs than the enumeration of 1 subsample. The greatest chance for falsely reporting the absence of SCPs was when <10 SCPs/gDM were measured in fewer than 10 subsamples. We recommend that a best practice for SCP enumerations is a minimum of 10 subsamples, with the flexibility to add subsamples as needed. We acknowledge that enumerating multiple subsamples per site is time and resource intensive, however, the statistical advantages measurement precision affords outweigh the costs.

## 2.2 Introduction

Spheroidal carbonaceous particles (SCPs) are only produced by the anthropogenic, high temperature combustion of fossil fuels (coal and fuel oil) (Wik & Renberg, 1996). SCPs are preserved in lacustrine, estuarine, and riverine sediments and are frequently used as indicators of anthropogenic impacts on the environment or to provide chronology for cores based on regional fossil fuel combustion history. SCPs are easily identifiable due to their unique black and spheroidal morphology which distinguishes them from geogenic sediments and most other fly ash materials (Rose, 2008; Rose et al., 1999). SCPs are concomitant with toxic trace metals (Boyle et al., 1998; Deonaraine et al., 2023; Larsen, 2000) and carcinogenic polycyclic aromatic hydrocarbons (Agency for Toxic Substances and Disease Registry, 1996; Barst et al., 2017; Rose & Rippey, 2002) which can have damaging impacts on human and environmental health.

Little work has sought to understand how SCP measurement uncertainty affects site-level interpretations of anthropogenic environmental impacts. Rose found that in laboratory standardized sediments, the precision of the mean SCP concentration calculated by enumerating SCPs in a set of 3 sediment trials was lower than when enumerating SCPs in a set of 15 sediment trials (Rose, 2008). Rose also found that for the same number of trials, SCP measurements in sediments of low SCP concentration have greater error than when enumerating SCPs in sediments of high SCP concentration (1990, 1994). In this context, trial refers to the counting of SCPs, where one trial means one count from one sediment sample, or ten trials means counting ten subsamples from the same sediment sample. However, a publication proposing a method for calculating or reporting the precision of SCP concentrations has not been presented, even though such a methodology has been published in related fields for sedimentary pollen (Comtois et al., 1999)

foraminifera (Kemp et al., 2020), macroinvertebrates (Doberstein et al., 2000), and charcoal (Schlachter and Horn 2010, Anderson et al. 2022), among others.

Previous analysis of enumeration methodologies similar to that of SCPs have consistently found that single subsamples provide an imperfect picture of overall sedimentary concentrations. In counting benthic macroinvertebrates, Doberstein et al. (2000) found that when a subset of only 100 organisms were counted out of the entire sample, the final metrics were much more variable than when the entire sample or when >100 organisms were counted. Variance increases with decreasing sample size. Smaller sample sizes cannot effectively or accurately distinguish if variability in the final measurement is an artifact of true site variability or the result of error introduced through the sampling method (Doberstein et al., 2000).

When quantifying sedimentary charcoal, Schlachter and Horn (2010) found that macroscopic particles are not homogeneously distributed among horizontal layers in sediment cores. While large scale changes in charcoal concentration were similar for all subsamples within the same horizontal layer of a core, small scale changes did not follow the same overall trend. They concluded that high-resolution inferences based on charcoal concentrations in a single subsample from a core may not be an accurate reflection of the charcoal abundances for that horizon (Schlachter & Horn, 2010). Anderson et al (2022) further confirmed the spatial heterogeneity of charcoal particle deposition within sedimentary cores. This lack of homogeneity requires additional subsamples to adequately capture charcoal abundances for a single horizon (Anderson et al., 2022). SCPs could be expected to behave similarly to charcoal particles in sediment stratigraphy. Therefore, a single subsample from a core may not provide an accurate representation of the theoretical mean of SCPs for that section, and any chronologic interpretations or inferences about anthropogenic impacts may be proportionally skewed. Enumeration methods in these and

other fields follow the mathematic law of large numbers, which states that as the number of replicate trials is increased, the average of the results approaches the theoretical mean (P. L. Hsu & Robbins, 1947). Despite this insight, common practice of SCP quantification (Rose, 1994; Wik & Renberg, 1996) remains reliant on the assumption that enumerating a single sediment sample is representative of the theoretical mean at a given site or time interval in a sediment record (Barst et al., 2017; Bowman & Harlock, 1998; Curtis et al., 2023; Inoue et al., 2022; Larsen, 2000; Ljung et al., 2022; Rose et al., 2012; Swindles, 2010). No additional studies have addressed how SCP concentration affects measurement error nor have any adopted the practice of enumerating SCPs in replicate trials.

We address this knowledge gap by applying new techniques to SCP enumeration. We enumerated multiple subsamples each from riverine sediment sites impacted by coal combustion. We then used a bootstrapping method that simulated a range of trials to approximate the sites SCP theoretical mean. We use the simulations to characterize the effect that the number of trials has on the precision of mean SCP concentrations and on measurement confidence intervals, which are critical to statistically interpret changes in SCP concentrations across sites or between time intervals in a sediment record. We also contextualize our findings within the literature, note the implications of our findings for SCP studies, and make recommendations for future analyses.

## **2.3 Materials and Procedures**

### **2.3.1 SCP quantification**

Surface sediment samples (n=14) were collected from the Coosa River in Alabama, United States in December of 2021 (Herron, 2022). Samples reflect sediments deposited from 2019 to the date of collection (Orndorff, 2021). Sediment samples were freeze-dried (Labconco™ 710612000) overnight at -80 °C and 1.2 mbar before being homogenized. Each of the 14 sediment samples were divided into 30 subsamples with each weighing (VWR-205AC/CAL) roughly 0.5 g and placed in 15 mL high density polyethylene centrifuge tubes (Globe Scientific, Item Number 6269) (Figure 2.1.a). Sediments were subjected to serial digestions in sodium hypochlorite (2.5%) (Clorox) and sodium hexametaphosphate (1M) (Thermo Fischer Scientific) (Ali et al., 2009). SCPs were quantified using a stereomicroscope at 20-22 times magnification (Nikon SMZ445) according to the characteristics described by Rose (2008) and Wik and Renberg (1996). SCP concentrations are reported as the number of SCPs per gram of dry mass of sediment (SCPs/gDM). SCP counts refer to the number of SCPs found in a subsample. To minimize error, subsamples from the same site were digested concurrently and a single analyst counted SCPs for all subsamples. No SCPs were counted for site A1, so it has been excluded from the following analyses.

### 2.3.2 Bootstrapping

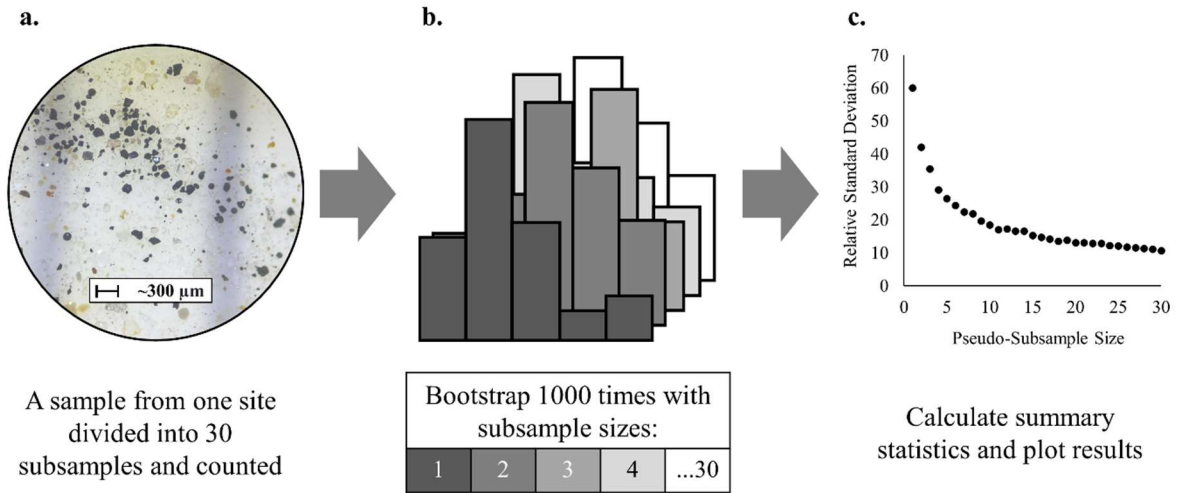


**Figure 2.1** Conceptual diagram of the bootstrapping workflow used in this study. **a.** One sediment sample is divided into 30 subsamples and spheroidal carbonaceous particles (SCPs) are counted for each. **b.** Concentrations are bootstrapped with pseudo-subsample sizes at integers between 1 and 30 to generate new pseudo-sample SCP concentrations. **c.** Summary statistics from each bootstrapped pseudo-sample are used to analyze trends in the data as a function of pseudo-subsample size.

The nonparametric bootstrapped data for this study was generated using SAS® OnDemand for Academics software, Version 3.81 (Enterprise Edition) of the SAS System for Linux. Copyright © 2012-2020 SAS Institute Inc. Subsample SCP concentrations (Figure 2.1.a) were bootstrapped using random sampling with replacement to generate pseudo-subsampled SCP concentrations for subsample sizes between 1 and 30 (Figure 2.1.b). Subsample size refers to the number of trials conducted per site. Pseudo-samples or pseudo-subsamples refer to the bootstrapped SCP concentrations, whereas raw samples or raw subsamples refer to initial SCP concentrations calculated by the researcher. Raw and pseudo-SCP concentrations were classified by a logarithmic scale. Summary statistics, including the population mean, standard deviation, 95% confidence intervals, and the relative standard deviation (RSD), were recorded for each

interval (Figure 2.1.c). The relative standard deviation was calculated for pseudo-subsamples and raw samples as

$$RSD = \frac{\sigma}{\mu} \times 100$$

Wherein:

$RSD$  = relative standard deviation

$\sigma$  = population standard deviation

$\mu$  = population mean

## 2.4 Assessment

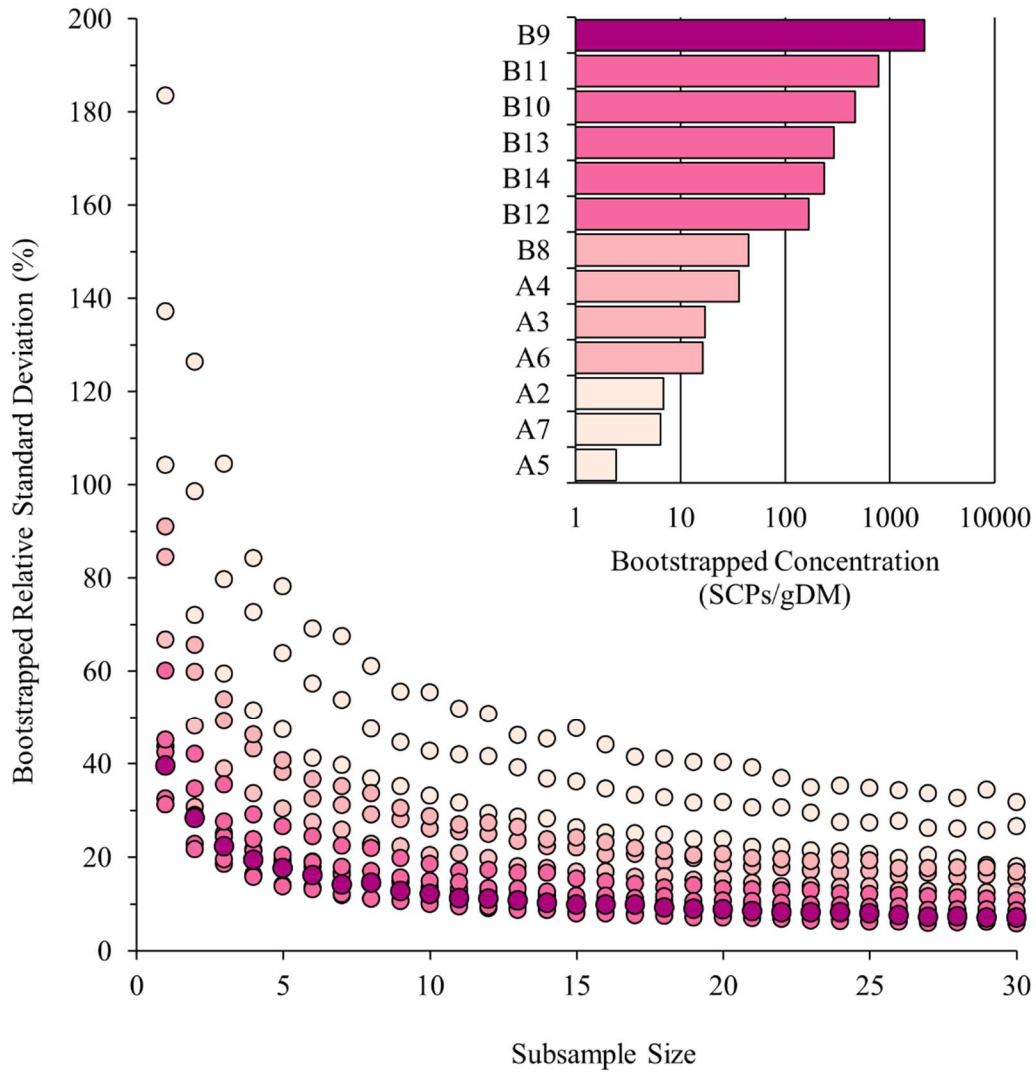
The summary statistics for raw samples and pseudo-samples for each site are presented in Table 2.1. The mean SCP concentrations in raw samples at the sites studied herein ranged between 0 (site A1) and 2141 SCPs/gDM (site B9) and were comparable to SCP concentrations in published literature (Figure 2.5; also see Supplementary Information). Sites were classified by the average mean SCP concentration of bootstrapped samples logarithmically as low (<10 SCPs/gDM), moderate (10-100 SCPs/gDM), high (100-1000 SCPs/gDM), or very high (>1000 SCPs/gDM). For all sites, the differences between the means calculated from the raw samples and pseudo-samples are small (Table 2.1) but the magnitudes of the RSDs are larger for the raw samples. For each site, the RSDs calculated from raw sample concentrations are 5 to 6 times greater than the RSD from the pseudo-samples, which is a reasonable difference considering the bootstrapped RSD is averaged over 1000 iterations.

**Table 2.1** Summary statistics for raw and bootstrapped spheroidal carbonaceous particle (SCP) concentration data. Means and standard deviations (SD) are reported as the number of SCPs per gram of dry mass of sediment (SCPs/gDM), and the number of times 0 SCPs were counted (# Zeros) are reported as the number of subsamples for each site in which no SCPs were found.

	Raw Samples				Bootstrapped Pseudo-samples		
	Mean (SCPs/gDM)	SD (SCPs/gDM)	RSD (%)	# Zeros	Mean (SCPs/gDM)	SD (SCPs/gDM)	RSD (%)
B9	2141	825	39	0	2140	150	7
B11	778	245	32	0	779	45	6
B10	467	151	32	0	467	27	6
B13	294	126	48	0	294	18	6
B14	235	111	47	0	235	20	9
B12	168	100	59	0	169	18	11
B8	45	19	43	1	45	4	8
A4	37	34	92	4	36	6	17
A3	18	14	81	4	17	3	15
A6	16	11	67	3	16	2	13
A2	7	7	104	13	7	1	18
A7	6	9	138	16	6	2	27
A5	2	4	174	21	2	1	32

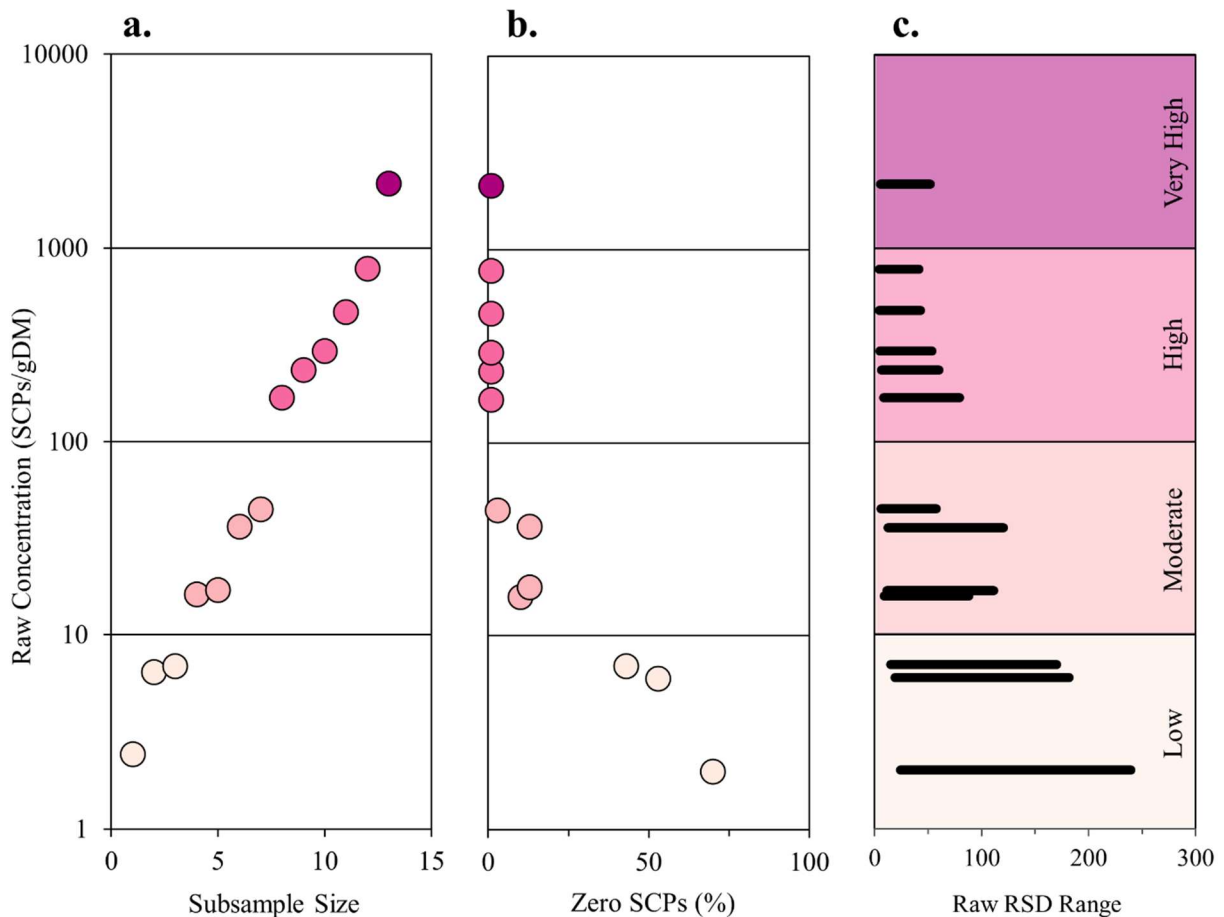
Figure 2.2 shows the relationship between the RSD and bootstrapped subsample size for pseudo-subsamples at each site. Sites with low SCP concentrations (0-45 SCPs/gDM) showed higher relative standard deviations for all subsamples than sites with high SCP concentrations (168-2141 SCPs/gDM). RSDs were found to be inversely related to pseudo-subsample sizes and SCP concentrations. As pseudo-subsample sizes and SCP concentrations increased, RSDs decreased (Figure 2.2), providing some evidence that the bootstrap data converged. Higher RSDs

were observed in sites with fewer than 10 SCPs/gDM (sites A2, A7, and A5) compared to sites with higher concentrations of SCPs for all pseudo-subsample sizes.



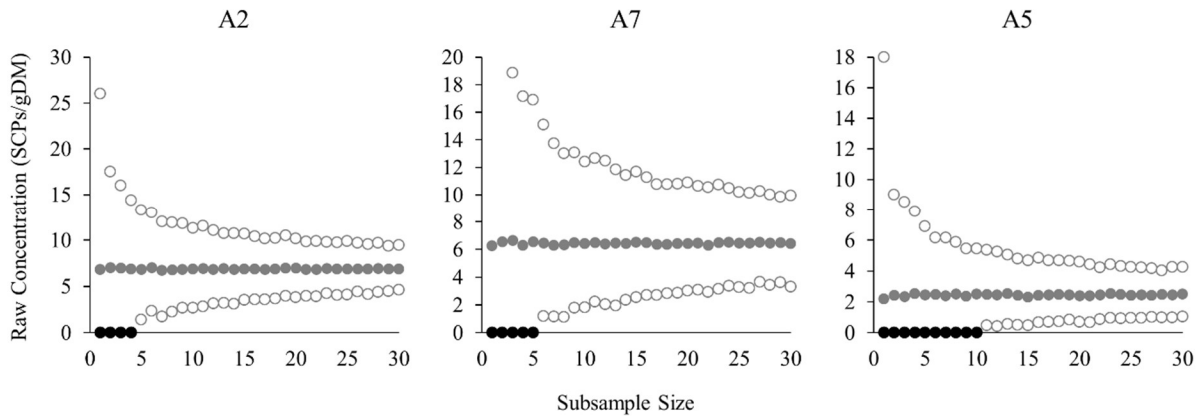
**Figure 2.2** The bootstrapped means and relative standard deviations (RSDs) for each sample. Site classifications are divided logarithmically. Samples with higher concentrations of spheroidal carbonaceous particles (SCPs) tend to have lower RSDs than samples with lower concentrations of SCPs. RSD decreases with increasing subsample size.

Figure 2.3 shows the relationship between SCP concentration, pseudo-subsample size, the proportion of subsamples with zero SCPs counted, and the RSD range for each site. Subsamples for sites with 0-100 SCPs/gDM had the potential to have no SCPs when analyzed, even though SCPs were present for that site (Figure 2.3b). The probability of a subsample having no SCPs decreases with increasing SCP concentration. All samples with SCP concentrations greater than 100 SCPs/gDM showed a 0% probability of zero SCPs in a subsample, meaning that all subsamples had at least 1 SCP identified. Samples with <100 SCPs/gDM showed a wider RSD range than samples >100 SCPs/gDM, which is also reflected in Figure 2.2.



**Figure 2.3 a.** Raw sample means compared to b. the percentage probability of any of the raw sample counts having zero spheroidal carbonaceous particles (SCPs) and c. each site’s relative standard deviation (RSD) range. Samples with lower SCP concentrations are more likely to have subsamples with no SCPs and wider RSD ranges than samples with higher SCP concentrations.

Sites with less than 10 SCPs/gDM exhibit the widest range of deviation from the mean and the highest probability of counting zero SCPs even though SCPs are present for that sample. Figure 2.4 shows the 95% confidence intervals around the means for sites with less than 10 SCPs/gDM: A2, A7, and A5. For a subsample size of one, samples with fewer than 10 SCPs/gDM have no confidence that the minimum concentration is not zero. For site A5, with a mean of 2 SCPs/gDM, there is no confidence that the minimum SCP concentration is not zero for the first 10 subsamples.



**Figure 2.4** Bootstrapped upper and lower 95% confidence intervals for samples with <10 spheroidal carbonaceous particles (SCPs) per gram of dry mass of sediment (SCPs/gDM). Samples with less than 10 SCPs/gDM at 1-10 subsamples can have no confidence that the minimum concentration is not 0. Quantifying SCPs in subsample sizes greater than one gives confidence in the presence or absence of SCPs for samples with less than 10 SCPs/gDM.

## 2.5 Discussion

### 2.5.1 Quantifying SCPs with subsampling

The overall goal of counting SCPs in a sample is to use the data as a proxy to quantify human-impacts on the environment. Naturally, data and its interpretation are constrained by measurement uncertainty. Our analyses show quantifying SCPs in 30 subsamples trends toward a theoretical mean for each site. Importantly, samples with low and moderate SCP concentrations have higher probabilities of zero SCP counts in any given subsample, which could lead to misinterpretations of anthropogenic impacts indicated by the first occurrences of SCPs in sediment records. In 1990 and 1994, Rose found that generally, for the same number of trials ( $n=15$ ), the mean of samples with higher concentrations of SCPs is more precise than that of samples with lower concentrations. While the SCP concentrations for Rose's studies were higher (7687-70544 SCPs/gDM) than those studied here, we confirm Rose's conclusions. For samples with low ( $<10$  SCPs/gDM) concentrations, the RSD was higher than that of samples with  $>100$  SCPs/gDM (Figures 2.2 and 2.3).

We also found that subsampling is critical for samples with  $<100$  SCPs/gDM. Increasing the number of trials, or the subsample size, better approximated the theoretical mean and provided a more robust dataset on which to base interpretations about changes in SCP concentrations across sites. Altogether, these results recommend against the common practice of enumerating one subsample to represent the mean SCP concentration for a site or section of a core. Further, a more accurate population mean can be approximated by increasing the number of subsample trials for each sample, particularly for samples with low or moderate SCP concentrations.

Based on the results of the samples analyzed in this study, we set a minimum subsample size of 10 as best practice for future sediment SCP quantifications, with the recommendation to

add subsamples if the mean of SCPs is low. This threshold is the minimum number of subsamples required to achieve confidence above zero for sites in this study (Figure 2.4). The 10-subsample threshold for SCP quantification is likely a prudent guide for future researchers, however, selecting subsample sizes is also dependent on the concentrations of SCPs in the sample.

For samples with high and very high SCP concentrations, the increase in measurement precision beyond a subsample size of 10 is minimal (Figure 2.2). Sites with <10 SCPs/gDM showed the largest increase in precision when quantifying more than one subsample, with the precision of some sites increasing by an order of magnitude. We found that the benefit of quantifying 5 to 10 additional subsamples on SCP measurement precision was worth the time and resources required to count additional subsamples. Therefore, particularly for samples with low to moderate SCP concentrations, it is important to consider the effect of subsample size on count precision when designing and executing experiments.

The sediments in this study are fluvial in origin, which could cast doubt on the universality of our conclusions for global SCP analyses that primarily focus on lacustrine sediments. However, we found that SCP concentrations in fluvial sediments have a wide range of concentrations (0-2141 SCPs/gDM) comparable to those in published literature (Figure 2.5). To this end, despite the fluvial sourcing of the sediments and SCPs analyzed in this study, we assert that our conclusions are applicable to the broader body of SCP research in the literature.

Though we suggest replicate subsampling as a prudent means of establishing SCP concentration confidence and precision, we also acknowledge that it is time and resource consumptive. Indeed, we speculate that the reason replicate subsampling has not become the norm is due to the confluence of assumptions regarding the representativity of single subsample measurements, as well as the time-cost of undertaking replicates (Anderson et al., 2022). As an

example, it took this research team approximately 3-5 days of batch preparation and 10 to 15 minutes of focused attention at the microscope to identify and count SCPs for each subsample. Extrapolated to the 420 subsamples presented here, the quantification of SCPs amounts to 70 to 105 hours of microscope time in addition to batch preparation time. Clearly, it is beneficial to balance quality data with the cost of analysis time and researcher fatigue.

### **2.5.2 SCPs and the Anthropocene**

SCPs are globally dispersed via atmospheric circulation and accumulate in sediments over time (Inoue et al., 2022; Larsen, 2000; Rose, 2015; Rose et al., 2020; Schneider et al., 2021; Thomas, Tetzner, et al., 2023; Vachula et al., 2023; Wik & Renberg, 1996) (Figure 2.5). On the global scale, changes in industrialization are recorded with virtual synchronicity in sediment records despite local variability. The onset of industrialization in the nineteenth century (Larsen, 2000; Ljung et al., 2022; Rose & Appleby, 2005) and the global increase of fossil fuel consumption in the 1950s (Head et al., 2022; Inoue et al., 2022; Rose, 2015; Waters et al., 2023) are both recorded by the first appearance or an increase in concentration of SCPs.

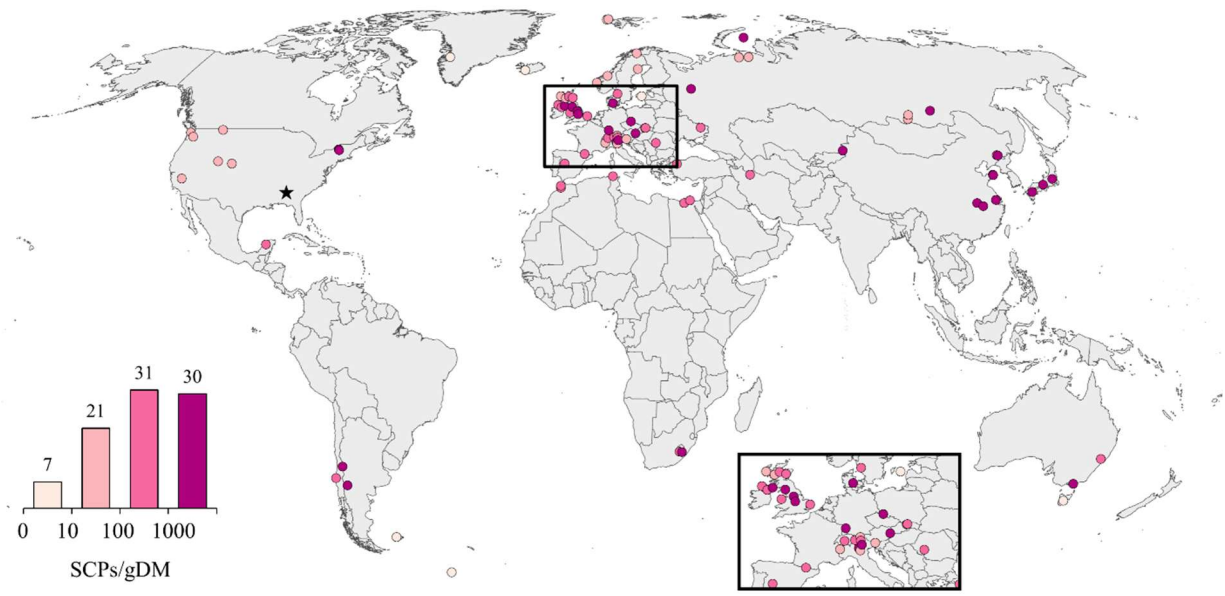


**Figure 2.5** Sites of spheroidal carbonaceous particle (SCP) enumeration (n=89); the maximum SCP concentration for each site is classified using a logarithmic scale. The shade of each class darkens with increasing SCP concentration. The numbers above the bar graph note the number of sites per class. The star represents the location of the samples for this study. SCP concentration and location data are modified from Rose, 2015 with additional sites from Barst et al., 2017; Curtis et al., 2023; Fiałkiewicz-Kozieł et al., 2023; Han et al., 2023; Himson et al., 2023; Inoue et al., 2022; Kaiser et al., 2023; McCarthy et al., 2023; Rose et al., 2020; Schneider et al., 2021; Stegner et al., 2023; and Thomas, Vladimirova, et al., 2023. Classifications and additional references for each study are listed in Table S.2.1 in Appendix 1.

SCPs have been proposed as an ideal stratigraphic marker to define the beginning of the Anthropocene Epoch due to their relationship with fossil fuel combustion and industrialization (Rose, 2015; Waters et al., 2016). The beginning of the Anthropocene Epoch is proposed to align with the period of rapid industrialization in the 1950s (Head et al., 2022; Steffen et al., 2015). This period, henceforth referred to as the “Great Acceleration”, coincides with rapid increases in SCP concentrations measured in global sediment records (Steffen et al., 2007). There is general agreement that global SCP concentrations were lower in sediment records before the 1950s as compared to the observed exponential increase in SCP concentrations during the Great Acceleration (Rose, 2015). Therefore, the positive deviation of SCP concentrations above a low

or zero value background in sediment records has important implications for identifying the timing of human-caused environmental impacts.

SCP quantification is regularly used to date the timing of regional and global industrialization events in ice or sediment records (Barst et al., 2017; Garcés-Pastor et al., 2023; Inoue et al., 2022; Ljung et al., 2022; Rose et al., 2012; Rose & Rippey, 2002; Stringer et al., 2014; Thomas, Tetzner, et al., 2023; Waters et al., 2023). Oftentimes, the earliest sections in a core have no or very few SCPs (Figure 3 in Rose, 2015). Figure 2.5 shows a summary of the available and published SCP quantification data. Roughly 31% of these published sites have SCP concentrations classified in our scheme as low or moderate (Bindler et al., 2001; Cameron et al., 1993; Kaiser et al., 2023; Koinig et al., 2002; Korhola et al., 2002; Landers et al., 2008; Larsen, 2000; Muri et al., 2006; Pla et al., 2009; Renberg & Wik, 1985; Rose, 1996, 2015; Rose et al., 1998, 1998, 2004, 2012; Solovieva et al., 2005; Thies et al., 2011). Based on our findings, it is probable that there are cases where subsampling would reveal trends toward a theoretical mean that is different from what a single enumeration reveals. Samples with low-to-moderate concentrations inherently have an increased probability of a zero-SCP count, which may shift the timing of inferred anthropogenic impacts for the site. By only enumerating one subsample for each site or section of a core, the measurement precision, confidence intervals, and statistical interpretations are limited.

## 2.6 Comments and recommendations

SCPs are a useful sedimentary indicator of anthropogenic environmental contamination from coal- or oil-fired power plants (Rose, 2015). However, SCP enumeration, like similar employments in other related fields, must be bound by uncertainty in the measurement. The precision of a sample's mean increases as the number of subsamples increases, allowing for better approximations of that sample's theoretical mean. However, the recommended number of subsamples is not static and depends on the level of precision and accuracy desired for each project. We recommend as a best practice in SCP quantification to use a minimum of 10 subsamples, with flexibility to increase subsamples as needed for samples with low or moderate SCP concentrations. The practice we recommend constrains the uncertainty of the measurement and protects against falsely reporting zero SCPs when there are SCPs present. The ability to calculate the precision of reported SCP concentrations also allows statistical comparisons between samples or sites and improves the rigor of analysis. It has been established that increasing sample sizes increases measurement precision and allows for a better encapsulation of the theoretical mean. As SCPs are often employed as sensitive indicators of regional or global periods of industrialization, particle concentrations must be precise to accurately represent the anthropogenic activities at the time of SCP deposition. Therefore, our recommendation of enumerating a minimum of 10 subsamples per sample provides the necessary precision and confidence to ensure any site interpretations are reflective of the samples theoretical mean.

## **Chapter 3: Comparing sedimentary impacts of coal combustion from active and inactive coal fired power plants**

Authors: Emma D. Henderson, Ann S. Ojeda, and Richard S. Vachula

This chapter was edited after 4/1/2024 to be submitted for publication in Science of the Total Environment.

### **3.1 Abstract**

Coal combustion is a globally dominant energy source, responsible for the production of millions of tons of coal combustion products (CCPs). CCPs include particulates such as fly ash, bottom ash, and slag; organic compounds such as polycyclic aromatic hydrocarbons (PAHs); and toxic elements such as arsenic, lead, chromium, and others. In the U.S., many coal fired power plants (CFPPs) are closing or switching to other fuel sources. Additionally, many sites are closing CCP impoundments, which can pose threats to human and environmental health. Of these impoundments, most have been rated satisfactorily by the U.S. EPA, but many are fairly or poorly rated. While catastrophic failures of impoundment structures and toxic, passive leeching into ground and surface water garner much needed attention, satisfactorily rated impoundments are comparatively understudied. Here, we study the differing environmental impacts at an active CFPP relative to a legacy (or closed) CFPP, to better understand the future risks these facilities pose for the environment, even when closed. We use traditional proxies for CCP environmental impacts such as toxic metal enrichment and organic matter (OM) concentrations to compare both sites. We also employ a non-traditional proxy, spheroidal carbonaceous particles (SCPs), which are more commonly used to date sediment cores. SCPs are a unique CCP, in that they are only produced by the high temperature combustion of coal or fuel oil and are easily identifiable under a microscope. We find minimal CCP impacts when analyzing metal enrichments or OM concentrations, but SCPs provide clear, unambiguous evidence for the presence of CCPs in sediments. SCPs provide evidence for the legacy of coal combustion; particles are still present in sediments after coal

combustion has ceased and the CCP impoundment has closed. As more CFPPs begin to phase out coal and close CCP impoundments, considerations should be made to minimize legacy impacts.

## 3.2 Introduction

Coal will remain a globally dominant fuel source into the mid-twenty-first century (EIA, 2023). In 2022, 68 million metric tons of coal combustion products (CCPs) were produced in the United States, and roughly 38% of the byproducts were disposed of in impoundments or landfills (American Coal Ash Association, 2022). The EPA classifies CCPs as fly ash, bottom ash, boiler slag, and flue gas desulfurization material that are produced in coal-fired power plants (CFPPs) (US EPA, 2023). Regulations limit the direct discharge of CCPs into the environment, but illicit spills and passive contamination of aqueous and solid waste still occur (Deonarine et al., 2023; Harkness et al., 2016; Vengosh et al., 2019). Contaminants in wastewater, ash, or surface runoff are mobilized into waterways by direct discharge, leaching, or groundwater infiltration (Deonarine et al., 2023). Numerous studies have found evidence of CCPs in surface and groundwater near CFPPs (Ruhl et al., 2012; Vengosh et al., 2012; Wang et al., 2022).

The impact of CCPs on the environment is frequently assessed using an environmental forensics approach wherein multiple lines of evidence are collected and evaluated. Sediments affected by CFPPs or CCPs are frequently enriched in fly ash particles, as well as toxic metals and organic materials (OM). Major constituents of CCPs typically include silicates, iron oxides, and aluminum oxides, with the relative concentrations of these constituents being directly related to the mineralogy and chemistry of the parent coal (Tiwari et al., 2014; Vassilev & Vassileva, 1996; Zielinski et al., 2007). Minor elemental constituents are calcium (Ca) and magnesium (Mg) with trace concentrations of chromium (Cr), nickel (Ni), arsenic (As), cadmium (Cd), antimony (Sb), and lead (Pb) (Deonarine et al., 2015; Tiwari et al., 2014; Zielinski et al., 2007). Most elemental concentrations are enriched in CCPs relative to their parent coals. Enrichment tends to be greater for fly ash than for slag or bottom ash, as these particles are smaller and have more surface area

for the condensation of toxic metals (Tiwari et al., 2014). Because CCPs are enriched in toxic metals, enrichment trends relative to pristine sediment, particularly ones that coincide with the CCP cocktail, are used as lines of evidence for CCP contamination (Dragović et al., 2013; Gopinathan et al., 2022; Munawer, 2018; Vengosh et al., 2019).

Like for toxic metals, OM signatures in CCPs reflect the parent coal (Ribeiro et al., 2014). Sediment can retain OM signatures from CCPs including organic compounds such as polycyclic aromatic hydrocarbons (PAHs) (Barst et al., 2017; W. T. Hsu et al., 2016; Lima et al., 2005; Lu et al., 2022), spheroidal carbonaceous particles (SCPs) (Rose, 2008; Swindles et al., 2015), and unburned coal (Bartoňová, 2015; Gopinathan et al., 2022; Külaots et al., 2004; Tripp et al., 1981). PAHs sourced from coal combustion and unburned coal have been found in the environment near CFPPs and have been used to trace the impact of CCPs in areas surrounding CFPPs (Ribeiro et al., 2014; Stout & Wasielewski, 2004).

Fly ash particulates have also been measured in sediments by measuring magnetic susceptibility (Cowan et al., 2013, 2017; Querol et al., 1994), the visual identification of fly ash (Alliksaar et al., 1998; Cowan et al., 2013; Wang et al., 2022), calculating metal enrichments relative to pristine sediments (Harkness et al., 2016; Ruhl et al., 2012), calculating isotope (e.g. boron and strontium) ratios that reflected coal as opposed to the native sediment (Harkness et al., 2016; Vengosh et al., 2019; Wang et al., 2022) or the enumeration of SCPs found in CCPs (Inoue et al., 2022; Larsen, 2000; Rose, 1994; Rose et al., 2012; Thomas, Tetzner, et al., 2023). SCPs directly reflect coal combustion impacts as a unique, easily identifiable particle only produced through the high temperature combustion of coal or fuel oil (Rose, 2008; Rose et al, 1999; Wik & Renberg 1996).

Many studies are concerned with CCPs found in the environment as a result of catastrophic or unmonitored CCP spills or CCPs leaking from impoundments (Harkness et al., 2016; Ramsey et al., 2019; Ruhl et al., 2010, 2012; Vengosh et al., 2019). In 2008, at the Tennessee Valley Authority (TVA) Kingston Fossil Plant, over 4.1 million cubic meters of coal fly ash were released into the environment (Ruhl et al., 2009). The primary contaminants of ecological concern were toxic elements such as As, selenium (Se), Boron (B), strontium (Sr), and barium (Ba) (Ruhl et al., 2010). Toxic element concentrations in sediments near Kingston Fossil Plant continued to be elevated years after the spill (Ramsey et al., 2019). An example of unmonitored CCP spills is Sutton Lake in North Carolina, located near the site of Duke Energy's Sutton CFPP and CCP impoundment (Vengosh et al., 2019). Here, as well as near the Kingston CFPP, trace metal enrichment in bottom sediments were indicators of CCPs in the lake.

In the U.S., there has been a shift away from coal combustion for energy production, and in recent decades, CFPPs have increasingly closed (Fritsch, 2021) or transitioned to other fuel sources (Aramayo, 2020). Although the accumulation of CCPs has diminished with decreasing coal combustion, the environmental legacy surrounding the impoundments is largely understudied, potentially due to their broadly stable condition. In 2015, the EPA evaluated CCP impoundments (n=555) in the U.S. and determined that the bulk are of satisfactory condition (43%). However, the remaining impoundments are either in poor (27%) or in fair (30%) condition, and as such, the long-term threat of environmental impacts from these impoundments is higher (Figure 3.1). The security of CCP impoundments is increasingly at risk due to the stressors of climate change. For example, Deonarine et al. (2023) found numerous CCP impoundments that will be at risk as climate change increases the likelihood and severity of hurricanes (n=22 impoundments) and floods (n=61 impoundments). Increasing storm events can release additional CCPs into the

environment, as investigated by Vengosh et al. (2019) who found evidence that hurricane-induced flooding increased the volume of CCPs in lake sediments above average values. The increasing threat of strong climate change caused natural disasters, along with the state of many CCP impoundments, highlights the need to understand baseline effects of CCPs on the environment prior to catastrophic events.

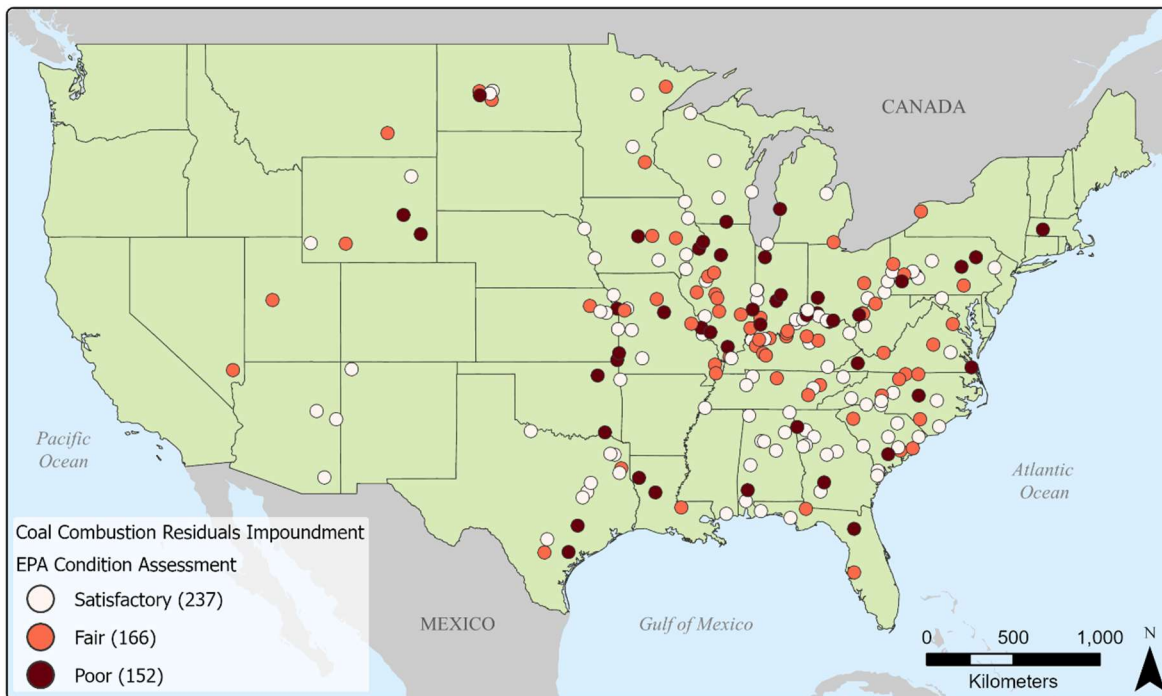


**Figure 3.1.** Coal combustion residuals impoundments in the contiguous United States as assessed by the U.S. Environmental Protection Agency (EPA). Impoundment assessment grades are either satisfactory (lightest shade), fair (medium shade) or poor (darkest shade). Data from U.S. EPA (2014).

Here we take a multiple lines of evidence approach to assess the potential for legacy environmental impacts of CCP impoundments. First, we investigate EPA-compliant CCP impoundments, which represent 43% of the impoundments nationwide, yet have not garnered much attention. Second, we compare sediment fingerprints from an active and a legacy (closed) CFPP. Evidence from SCPs, toxic metals, and OM provides insight into the long-term environmental impacts of CFPPs. SCPs, while used frequently as a paleolimnological tool for

dating sediments, are used herein as a novel proxy for CCPs in riverine sediments. Although CFPPs are frequently and increasingly closing or transitioning to non-coal fuel sources, CCPs will remain a potential environmental risk for years to come. Our approach provides a means of assessing the future fate and environmental impact of the CFPPs and their associated CCP impoundments.

### **3.3 Materials and methods**

#### **3.3.1 Study sites**

This study focused on two CFPPs in Alabama. Plant Gadsden is the northernmost plant. It has not burned coal since 2015, and therefore is referred to as the legacy CFPP site (Figure 3.2), however, it still hosts an ash impoundment that accumulated CCPs from its active regime between 1949 and 2015 (Alabama Power, 2020b). In 2018, the CCP impoundment at the legacy CFPP was closed-in-place in a manner that minimizes water infiltration into the cover and potential release of CCPs through the cover (Alabama Power, 2018a). Plant Gaston is the southernmost plant and is an active CFPP site (Figure 3.2). It has burned coal since 1960, and although 4 of 5 units transitioned to natural gas in 2016, coal combustion still occurs at the active site (Alabama Power, 2022). The impoundment at the active site ceased receipt of CCPs in April of 2019, and has begun the process to close the impoundment with the ash in place (Alabama Power, 2020a). The CCP impoundments at both the legacy and active CFPP sites are unlined (Alabama Power, 2016, 2018c).

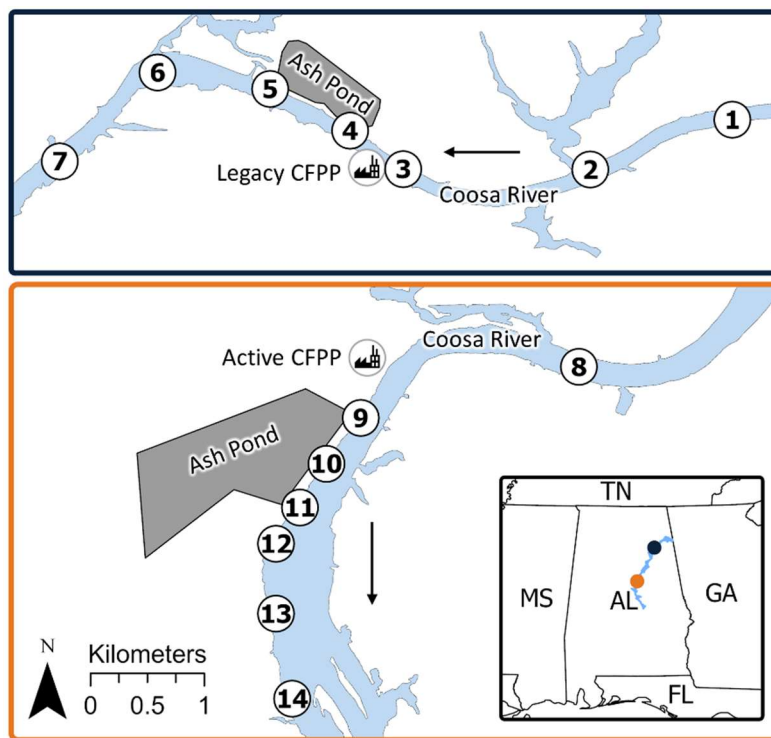


**Figure 3.2.** Study sites (n=14) in the Coosa River, AL, U.S. Northernmost sites 1 to 7 (Top) are near the legacy coal fired power plant (CFPP) and coal combustion product (CCP) impoundment (Ash Pond). Sites 8 to 14 (Bottom) are near the active CFPP and ash pond. The flow direction of the Coosa River is depicted with arrows. Previous work dating sedimentation rates in the Coosa River suggest these samples span approximately two years of accumulation (Orndorff, 2021).

### 3.3.2 Sediment collection and analysis

Surface sediments (n=14) were collected from the Coosa River, AL, U.S. near the two sites in December of 2021 (Figure 3.2). Sediments were kept on ice after collection and stored at 4 °C prior to analysis (Herron, 2022). Instruments were cleaned with acetone and 18.2 Ω water between sites to limit cross contamination. Sediments were prepared for metal analysis according to EPA Method 200.2. Metal analysis was conducted according to EPA Method 3052 by the University of Georgia’s Laboratory of Environmental Analysis. Inductively coupled plasma mass spectrometry (ICP-MS) was used to quantify vanadium (V), Cr, iron (Fe), Mg, Ca, Ni, As, copper (Cu), selenium (Se), strontium (Sr), molybdenum (Mo), Sb, Pb, and thallium (Tl). NIST Standard Reference

Material 1633c: Trace Elements in Coal Fly Ash was analyzed alongside sediments in triplicate (Herron, 2022). Measured concentrations of Se at several sites were below the detection limit, therefore Se is not included in further analyses.

To quantify SCPs, freeze-dried sediment samples were homogenized before being divided into 30 subsamples per site. Sediments were digested with household bleach (2.5%) and sodium hexametaphosphate (1M) to remove organic matter and deflocculate clays respectively (Ali et al., 2009). SCP enumeration was done using a stereomicroscope according to identification criteria established by Rose (2008) and Wik and Renberg (1996) and concentrations were recorded as the number of SCPs per gram dry mass (SCPs/gDM) (Figure S.3.1). One analyst quantified SCPs in all subsamples, and subsamples from each site were digested together to reduce error and cross contamination. SCP concentrations for each site are listed in Table S.3.1.

Loss on ignition (LOI) was performed on approximately 2.0 g of freeze-dried sediment from each site. Sediments were weighed after freeze drying, following combustion in a muffle furnace at 550°C for 2 hours, and again following combustion at 950°C for 4 hours. Sediment weights following each step were used to calculate percentages of organic matter ( $OM\% = \% LOI$  at 550°C), calcium carbonate ( $CaCO_3\% = \%LOI$  at 950°C  $\times (100/44)$ ), and the residual lithics and ash ( $LA\% = 100 - OM\% - CaCO_3\%$ ), including SCPs (Heiri et al., 2001; Vachula et al., 2017). Percent OM is listed for each site in Table S.3.1.

### **3.3.3 Statistics**

Reported SCP values were bootstrapped using random sampling with replacement to generate a new average of the 30 manually counted subsamples. The nonparametric bootstrapped

data for this study was generated using SAS® OnDemand for Academics software, Version 3.81 (Enterprise Edition) of the SAS System for Linux. Copyright © 2012-2020 SAS Institute Inc.

The 2-tailed correlation matrix was generated using GraphPad Prism Version 9.2.0(332) for Windows 64-bit, GraphPad Software, Boston, Massachusetts, USA, [www.graphpad.com](http://www.graphpad.com). When generating the correlation matrix, correlation coefficients were computed for every variable pair. Statistical significance is reported as the p-value ( $p$ ) while the strength and direction of the relationship is reported as the coefficient of determination ( $r^2$ ).

### **3.4 Results and discussion**

#### **3.4.1 Relationships between SCPs, toxic metals, and OM**

We observed spatial trends in SCP, toxic metal, and OM concentrations in relation to both the active and legacy CFPPs and their impoundments. SCP, toxic metal, and OM concentrations are all greater near the active CFPP than the legacy CFPP, with the highest concentrations of SCPs and OM at site 9, adjacent to the active CFPP. Toxic metal (excluding Mg, Cu, and Mo) concentrations are higher near the active CFPP than the legacy CFPP. SCP concentrations are a maximum of two orders of magnitude greater near the active CFPP than near the legacy CFPP. Though CCPs aren't being created at the legacy site, the environmental impact is evident even after coal combustion ceases. Other industrial sources could contribute to sediment metal or SCP concentrations, confounding the results observed here. However, both the legacy and active CFPPs are, or were, the only coal combusting facility within a radius of at least 15 kilometers. Furthermore, no coal combusting facilities were identified directly upstream from the sampling sites using the U.S. EPA's facility level information on greenhouse gases tool (FLIGHT) and their toxics release inventory (EPA, 2022, 2023). We posit, therefore, that SCP concentrations in these sediments only reflect inputs from the active or legacy CFPPs.

Elements frequently attributed to CCPs in the environment include Cr, Ni, As, Sb, and Pb (Deonarine et al., 2015; Tiwari et al., 2014; Zielinski et al., 2007). Sedimentary trace element concentrations were highest downstream of the active CFPP (Figure 3.3). Cr concentrations are highest at site 9, immediately downstream from the active CFPP. Further downstream, As and Pb are more concentrated in sediments at sites 12 and 13 (Figure 3.3). Sb concentrations are highest at the most downstream site 14. For the active CFPP, the effluent for the CCP impoundment enters

the river near site 11, which could explain the shift in respective metal concentrations (Alabama Power, 2018b).

It is known that ash from CFPPs can act as a carrier of toxic metals such as As, Pb, or Se (Querol et al., 1995). Additionally, weathering can be a geogenic source of trace metals in the environment that is not associated with CCPs. Natural OM can also be a scavenger for trace metals in the environment (Kinniburgh et al., 1999), and therefore the sorption to organic matter may, in part, explain trace metal abundance, again, outside of CCP influence. We might expect that concomitant production, fate, and transport of SCPs and trace metals in CCPs would result in similar distributions of both in the environment and overprint the geogenic signature. However, there is a dearth of research to understand the transport of metals into the environment directly through sorption onto SCPs. Through simple linear regression models, we found Fe generally explained concentrations of V ( $r^2 = 0.79$ ,  $p < 0.001$ ) and As ( $r^2 = 0.72$ ,  $p = 0.001$ ), most likely associated with weathering of shales in the region (Åhlgren et al., 2021; Butts & Gildersleeve, 1948). Fe also explained Cr ( $r^2 = 0.78$ ), when the notable outlier (site 9) was omitted from the regression. On the other hand, Pb was moderately explained by Fe ( $r^2 = 0.47$ ,  $p = 0.0063$ ), suggesting that the native sediment was not a predictable source of Pb (note that silicate minerals were not digested by the methods used here). SCPs predicted Cr concentrations ( $r^2 = 0.65$ ,  $p = 0.0004$ ). OM was related to Cr ( $r^2 = 0.57$ ,  $p = 0.0016$ ) and Fe ( $r^2 = 0.34$ ,  $p = 0.028$ ), but SCPs and OM were not related ( $r^2 = 0.21$ ,  $p = 0.0911$ ).

Little evidence exists that would suggest the fate and transport of SCPs and OM in the environment is linked. The bulk of work quantifying SCPs in sediments has focused on their application as a geochronological and general fossil fuel combustion indicator in sediment cores (Inoue et al., 2022; Larsen, 2000; Rose, 2015; Rose et al., 1998, 2012; Swindles, 2010). Therefore,

the link between SCPs and OM, as it pertains to source-to-sink transportation has not been explicitly investigated in the literature. SCPs and OM were not correlated across our sites. This correlation is bolstered by the relatively comparable OM% values of the legacy ( $\mu = 3.6\%$ ;  $\sigma = 2.10\%$ ) and active ( $\mu = 5.02\%$ ;  $\sigma = 2.08\%$ ) sample sites, despite stark differences in the range of SCP concentrations. Additionally, SCPs were not combusted with OM during the LOI analysis, indicating that the magnitude of SCP sedimentary concentrations had no effect on OM concentrations.

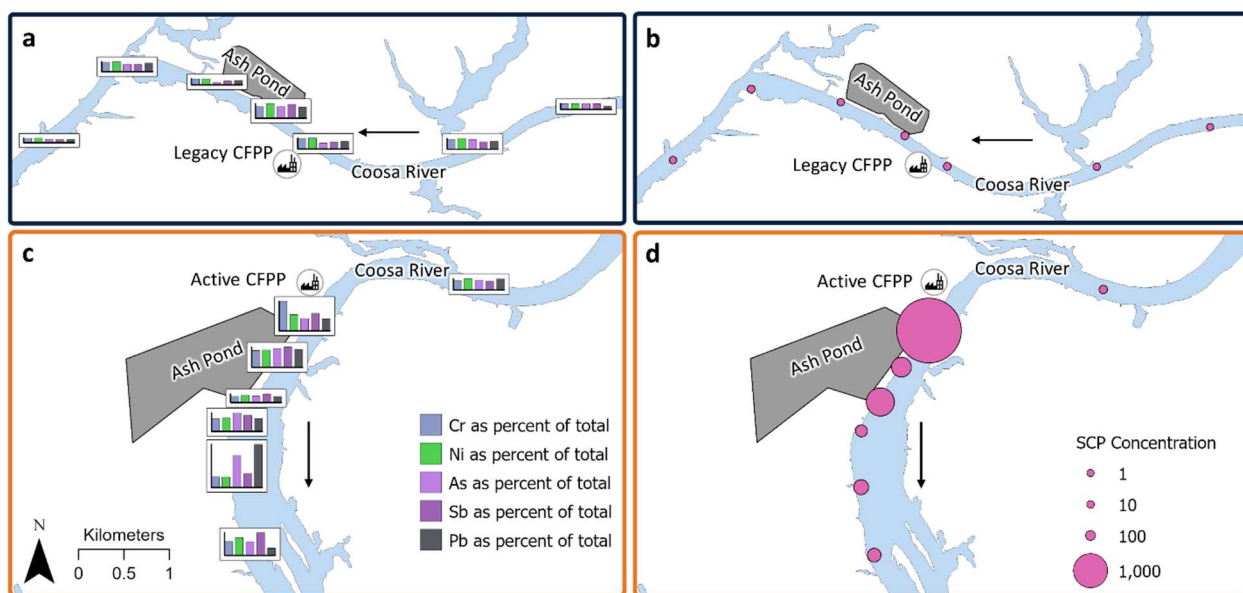


**Figure 3.3.** Metal concentrations in Coosa River sediments near the legacy (a) and active (c) coal fired power plants (CFPPs) and their coal combustion product (CCP) impoundments (Ash Pond). Bar charts show the respective proportions of chromium (Cr), nickel (Ni), arsenic (As), antimony (Sb), and lead (Pb) in sediments. Values for each metal are normalized as the percent the metal's concentration at each site contributes to the total metal concentration across all sites. Smaller bars represent smaller percentages and larger bars larger percentages. SCP concentrations in Coosa River sediments near the legacy (b) and active (d) CFPPs. Circle size increases with respect to mean site SCP concentrations (min = 0; max = 2138 SCPs/gDM). Site numbers follow those in Figure 3.2. The flow direction of the Coosa River is shown by the black arrows.

### 3.4.2 Metal enrichment compared to other CCP-impacted sites

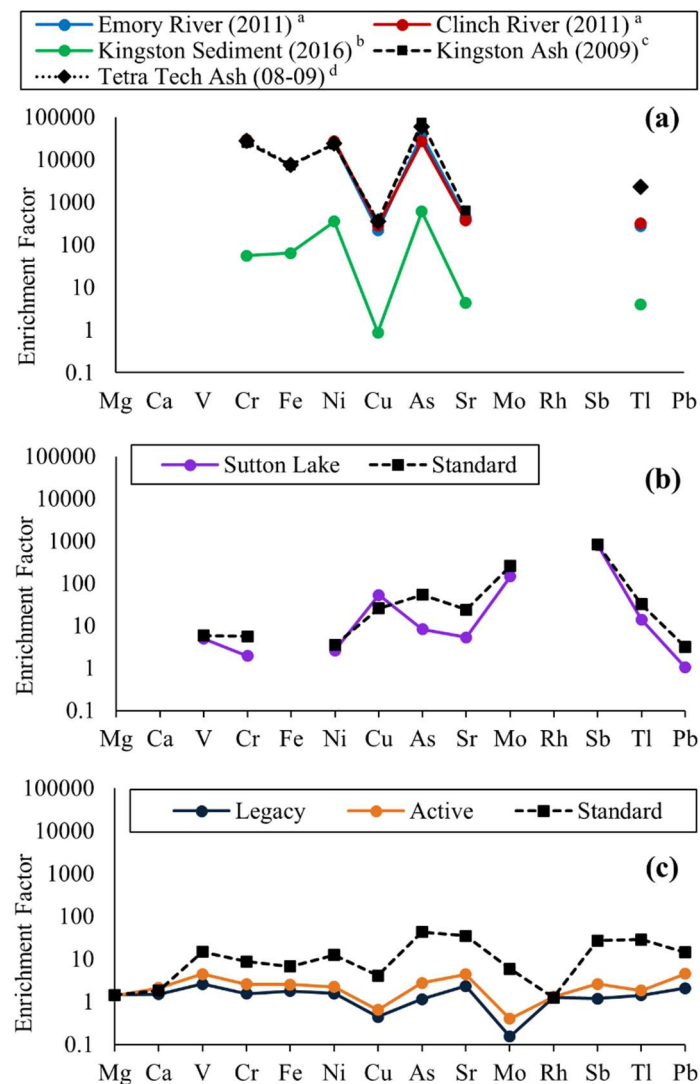
The enrichment of trace metals in sediments observed in this study was compared to the catastrophic 2008 Kingston, TN ash spill and the less obvious unmonitored CCP spills into Sutton Lake, NC (Figure 3.4). Enrichment factors were calculated for each metal as the ratio of the average concentration of that metal at all sites relative to its concentration at a pristine site for each study. For this study, the pristine site is the most upstream site 1. An enrichment of 1 means the concentration of toxic metals in sediment samples is equivalent to that in pristine sediments, while values greater than 1 represent an enrichment at the site and values less than 1 represent a depletion. A summary of the data used to generate these values is included in the supplementary data (Table S.3.2).

When the impoundment ruptured at the Kingston site, CCPs, specifically fly and bottom ash, were directly spilled into the Emory River, its tributaries, and moved downstream into the Clinch River (Ruhl et al., 2009). At the Kingston site, sediment collected in 2011 closely mimicked the magnitude and pattern of enrichment of the impoundment ash (Figure 3.4a, blue and red lines compared to the black lines). Additional sediment collected in 2016 showed a similar pattern, but the magnitude of enrichment decreased from 2011 to 2016 (Figure 3.4a, green line). Even though CCPs are directly spilled into Sutton Lake, like at Kingston, the volume of CCPs that entered the environment was much lower. Additional potential mechanisms of CCP transport into Sutton Lake include previous dumping practices or the historic impoundment of CCPs directly into Sutton Lake (Vengosh et al., 2019). The magnitude and pattern of enrichment in Sutton Lake followed that of the ash standard (NIST 1633c) (Figure 3.4b), but unsurprisingly, was lower in magnitude and differed in pattern from that of the Kingston Spill.

In this study, the fly ash standard (NIST 1633c) was enriched in all metals relative to the pristine site by a factor of 10 (Figure 3.4c, black line). The average enrichment for legacy and active CFPP sediments was near 1, suggesting minimal CCP contribution to sediment metal concentrations, although we have demonstrated above that the site-specific impact varies (Figure 3.3). While the metal CCP impact is minimal, the influence of CCPs is clearly seen through the fluctuations in sedimentary SCP concentrations. Additionally, the alignment between the patterns of enrichment for the CFPPs and the fly ash standard also suggest CCP impacts on the environment, even if at low magnitudes (Vengosh et al., 2019). For both the legacy and active sites, the highest enrichment is for Pb, V, and Sr. These elements are associated with CCPs, with V and Sr frequently elevated in CCP-impacted environments (Deonarine et al., 2023).

It is interesting that the same fly ash standard was used in the Sutton Lake study (Vengosh et al., 2019) as this study. For Sutton Lake sediments, the fly ash standard showed relative enrichments against the reference sediment (Waccamaw Lake) several orders of magnitude greater than what is observed in this study. In part, this can be attributed to the local mineralogy so that here, even the native sediment is enriched in trace metals, producing lower overall enrichment trends. In that case, it may suppress the enrichment signal from CCPs. For further analysis, the elemental composition of CCPs from both the active and legacy CFPPs would be a beneficial comparator. Sediments impacted by the Kingston, TN ash spill initially were enriched in trace elements at the same magnitude as the ash itself (Figure 3.4a, blue and red lines compared to black line). Years later, however, the magnitude of enrichment relative to the ash decreased.

**Figure 3.4.** Enrichment of metals in sediments impacted by coal combustion products (CCPs) and ash sourced from coal fired power plants (CFPPs) or a laboratory standard relative to metal concentrations in local pristine sediments. **(a)** Mean metal concentrations in sediments (solid lines) and ash (dashed lines) from the TVA Kingston Fossil Plant ash spill in TN compared to mean metal concentrations in pristine sediments from site 2 in Ramsey et al. (2019). Data references: <sup>a</sup>(Stojak et al., 2014); <sup>b</sup>(Ramsey et al., 2019); <sup>c</sup>(Ruhl et al., 2009); <sup>d</sup>(Tetra Tech EM Inc, 2009). **(b)** Mean metal concentrations from sediments (solid line) in Sutton Lake, NC and in NIST SRM 1633c (dashed line) compared to mean metal concentrations in sediments from pristine Lake Waccamaw, NC (Vengosh et al., 2019). **(c)** Mean metal concentrations in sediments (solid lines) near the Legacy CFPP (sites 2-7) and Active CFPP (sites 8-14) and in NIST SRM 1633c (dashed line) compared to pristine sediments from site 1 (this study).



### **3.5 Environmental implications**

Coal combustion, while an important means of global electricity generation, leaves a lasting impact on the environment, which has traditionally been measured by metal enrichment along with a suite of other potential proxies. We found the enrichment factors of metals for the legacy and active sites to be within the same order of magnitude, even though at the legacy CFPP coal combustion ceased in 2015 and the impoundment was closed in 2018 (Alabama Power, 2015).

While it is known that elevated levels of toxic metals can be from groundwater leaching of CCPs (Harkness et al., 2016), known groundwater leachates from impoundments studied herein, Mo and As for the active and legacy sites respectively, are not highly enriched in sediments. Therefore, while groundwater leaching could be occurring, leaching is not a primary mechanism for sedimentary enrichment of toxic metals in this study. It has also been found that atmospheric deposition from coal combustion can lead to metal enrichment in sediments (Wu et al., 2013). However, federal regulation in the U.S. and precipitators in smokestacks prevent the atmospheric transportation of particulate CCPs and toxic trace metals. Additionally, if SCPs and trace metals were deposited into the Coosa River from atmospheric transport, we would expect the greatest concentration of SCPs to be near the respective smokestacks, with concentrations decreasing linearly moving downstream (Vachula et al., 2023).

However, we found that SCP concentrations peak at two sites near both the active and legacy CFPPs. At both sites, SCP concentrations are initially greatest downstream of the CFPP, sites 4 and 9, and increase again downstream of the impoundment, sites 6 and 11. We propose two mechanisms of transport for SCPs and metals; surface runoff near the CFPPs and effluent from the impoundments. These mechanisms account for the initial and secondary SCP concentrations

at both the active and legacy sites and can explain the shift in trace metals at the active site from Cr being most concentrated near the CFPP to As and Pb being most concentrated downstream of the discharge structure.

While metals are often used as sedimentary proxies for CCP impacts (Ramsey et al., 2019; Ruhl et al., 2010; Vengosh et al., 2019; Wang et al., 2022), others (Rose et al., 1998; Yang et al., 2001) have noted that SCPs are able to provide a much more accurate sedimentary record of coal combustion than metals, as SCPs remain virtually unchanged once deposited, unlike metals. As demonstrated above, SCP peak concentrations aligned with those for metals, but SCP concentrations were not overprinted by geogenic or other anthropogenic signals. SCPs provide clear, unambiguous evidence for the presence of CCPs in the environment and were the best indicator of differences in CCP magnitude between the active and legacy sites. Indeed, the magnitude of SCPs in sediments near the active CFPP were 1 to 2 orders of magnitude greater than that of the legacy site. According to measurements of sedimentation rates, the ages of our sediment samples likely range from late 2019 to December 2021, meaning that for the legacy site, at least 4 years had passed since coal combustion ceased and 1 year since the CCP impoundment was officially closed (Orndorff, 2021). Despite years of time passing since coal combustion, we still observed SCPs downstream of the legacy site. If satisfactorily rated closed CCP impoundments and long-closed CFPPs show evidence of environmental impacts, the magnitude of expected impacts from active CFPPs and poorly or fairly rated active CCP impoundments is greater.

Of the several hundred satisfactory CCP impoundments across the contiguous U.S., many could be impacting the environment at equivalent magnitudes as those in this study. As we found, CCPs do not cease to appear in the environment when coal combustion ceases, and impacts persist

at closed, legacy sites. The results herein emphasize the importance of proper storage of CCPs and the urgent need for CCP generation, and therefore coal combustion, to decrease or cease. Even when coal combustion is obsolete, this legacy of contamination will remain. As more plants begin to phase out coal combustion and close CCP impoundments, considerations should be made to ensure legacy impacts are minimized.

## Chapter 4: Summary and Outlook

The overall goal of this work was to characterize the differences in sedimentary impacts between an active and a legacy CFPP using SCPs and other proxies. To utilize SCPs as a sedimentary proxy for CCP impacts, we developed a new enumeration method as described in Chapter 2. We defined SCP measurement uncertainty, and investigated how this uncertainty can affect total site concentrations and measurement error in our study and in global studies. In Chapter 3, we used the newly defined SCP enumeration method along with sedimentary metal and OM concentrations as proxies for CCP impacts. We found that CCP impacts were greater at the active CFPP when compared to the legacy site. We also found SCPs to be a better proxy for CCP impacts than the traditionally utilized metal enrichment factors.

This work could be furthered in several ways. First, a useful case study would be the SCP enumeration of a sediment core, particularly one dating at least to the 1950s. The boom of industrialization in the mid-twentieth century, dubbed the Great Acceleration (Steffen et al., 2015), correlates with a sharp increase in SCP deposition (Inoue et al., 2022; Rose, 2015; Waters et al., 2023). Numerous studies have measured this acceleration of SCP deposition, but, according to the findings in Chapter 2, many of the reported SCP concentrations could have errors. We found that out of 89 global SCP studies, 31% of the reported SCP concentrations may not reflect the theoretical mean of SCPs in the sediment at that site. These errors could shift the timing of inferred anthropogenic events that are often established based on SCP concentrations. These errors are particularly likely in samples with few SCPs. By only enumerating one subsample for each section of a core, the measurement precision, confidence intervals, and statistical interpretations are limited. Enumerating at least 10 subsamples from each section within a core would increase

precision and confidence in SCP concentrations, allowing for a better proxy of coal combustion during those years.

Second, the sediment record near the CFPPs examined in this thesis would offer an interesting perspective on correlating the deposition of SCPs with changes in local and national environmental regulations and policies. For example, both Inoue et al. (2022) and Schneider et al. (2020) found that sedimentary concentrations of SCPs correlated with increases or decreases of coal combustion and the addition of particulate or gaseous emission reduction devices. SCP concentrations near both CFPPs would also be expected to decrease when some or all combustion units were converted to burn natural gas instead of coal.

As global societies strive to meet new, more restrictive greenhouse gas requirements, understanding the legacy of coal combustion on the environment is extremely important. Numerous studies have investigated the effects of catastrophic spills or poorly rated impoundments, but few, if any, have investigated the environmental impacts and long-term fate of satisfactory CCP impoundments. Therefore, this study sheds new light on the more mundane, yet more prevalent, CCP impoundments. Additionally, very few studies have attempted to correlate the presence of SCPs and toxic metals as a more robust indicator of CCP environmental impacts. We found that for our sites, SCP concentrations measured using our new, proposed enumeration method were the strongest indicator of CCP impacts and agreed with toxic metal and OM concentrations. While the measured metal concentrations are not as extreme as at more catastrophic sites, CCPs are entering the environment at both the active and legacy CFPPs, as confirmed by SCP concentrations. Ultimately, a better understanding of CCP impacts near satisfactorily rated impoundments will be beneficial to future analyses and remediation efforts.

## References

- Agency for Toxic Substances and Disease Registry. (1996). *POLYCYCLIC AROMATIC HYDROCARBONS (PAHs) (ToxFAQs)*. U.S. Department of Health and Human Services. [https://www.epa.gov/sites/default/files/2015-04/documents/walter\\_atcdr\\_pahs.pdf](https://www.epa.gov/sites/default/files/2015-04/documents/walter_atcdr_pahs.pdf)
- Åhlgren, K., Sjöberg, V., Allard, B., & Bäckström, M. (2021). Groundwater chemistry affected by trace elements (As, Mo, Ni, U and V) from a burning alum shale waste deposit, Kvarntorp, Sweden. *Environmental Science and Pollution Research International*, 28(23), 30219–30241. <https://doi.org/10.1007/s11356-021-12784-2>
- Alabama Power. (2015). *Notification of Intent to Initiate Closure Plant Gadsden Inactive CCR Surface Impoundment Alabama Power Company Gadsden, Alabama*. <https://www.alabamapower.com/content/dam/alabama-power/pdfs-docs/company/how-we-operate/ccr/plant-gadsden/ash-pond/closure-and-post-closure/NOTIFICATION%20OF%20INTENT%20TO%20INITIATE%20CLOSURE.pdf>
- Alabama Power. (2016). *Liner Design Criteria 40 C.F.R. Part 257.71 Plant Gaston Ash Storage Surface Impoundment Alabama Power Company*.
- Alabama Power. (2018a). *Closure Plan for Existing CCR Surface Impoundment Plant Gadsden Ash Pond 40 CFR 257.102(b)*.
- Alabama Power. (2018b). *History of Construction for Existing CCR Surface Impoundment Plant Gaston Ash Pond*. <https://www.alabamapower.com/content/dam/alabama-power/pdfs-docs/company/how-we-operate/ccr/plant-gaston/ash-pond/design-criteria/History%20of%20Construction%20-%20Ash%20Pond.pdf>

Alabama Power. (2018c). *Liner Design Criteria 40 C.F.R. Part 257.71 Plant Gadsden Ash Pond*  
*Alabama Power Company.*

Alabama Power. (2020a). *Amended Closure Plan for Ash Pond* (p. 36).

<https://www.alabamapower.com/content/dam/alabama-power/pdfs-docs/company/how-we-operate/ccr/plant-gaston/ash-pond/closure-and-post-closure/Gaston%20Ash%20Pond%20Amended%20Closure%20Plan%20REV1%20April%202020.pdf>

Alabama Power. (2020b). *Plant Gadsden Timeline.*

<https://www.alabamapower.com/content/dam/alabama-power/pdfs-docs/company/compliance---regulation/public-meetings/One-Page-Plant-Gadsden-Timeline.pdf>

Alabama Power. (2022). *Integrated Resource Plan Summary Report (Summary Report 2022 IRP).*

Ali, A. A., Higuera, P. E., Bergeron, Y., & Carcaillet, C. (2009). Comparing fire-history interpretations based on area, number and estimated volume of macroscopic charcoal in lake sediments. *Quaternary Research*, 72(3), 462–468.

<https://doi.org/10.1016/j.yqres.2009.07.002>

Alliksaar, T., hörstedt, P., & Renberg, I. (1998). Characteristic Fly-ash Particles from Oil-shale Combustion Found in Lake Sediments. *Water, Air, and Soil Pollution*, 104(1), 149–160.

<https://doi.org/10.1023/A:1004918419356>

American Coal Ash Association. (2022). *Coal Combustion Product (CCP) Production & Use Survey Report 2022*. <https://aca-usa.org/wp-content/uploads/2023/12/2022-Production-and-Use-Survey-Results-FINAL.pdf>

- Anderson, L., Presnetsova, L., Wahl, D. B., Phelps, G., & Gous, A. (2022). Assessing reproducibility in sedimentary macroscopic charcoal count data. *Quaternary Research*, *111*, 177–196. <https://doi.org/10.1017/qua.2022.43>
- Aramayo, L. (2020, August 5). *More than 100 coal-fired plants have been replaced or converted to natural gas since 2011—U.S. Energy Information Administration (EIA)*. EIA. <https://www.eia.gov/todayinenergy/detail.php?id=44636>
- Barst, B. D., Ahad, J. M. E., Rose, N. L., Jautzy, J. J., Drevnick, P. E., Gammon, P. R., Sanei, H., & Savard, M. M. (2017). Lake-sediment record of PAH, mercury, and fly-ash particle deposition near coal-fired power plants in Central Alberta, Canada. *Environmental Pollution*, *231*, 644–653. <https://doi.org/10.1016/j.envpol.2017.08.033>
- Bartoňová, L. (2015). Unburned carbon from coal combustion ash: An overview. *Fuel Processing Technology*, *134*, 136–158. <https://doi.org/10.1016/j.fuproc.2015.01.028>
- Bindler, R., Renberg, I., Appleby, P. G., Anderson, N. J., & Rose, N. L. (2001). Mercury Accumulation Rates and Spatial Patterns in Lake Sediments from West Greenland: A Coast to Ice Margin Transect. *Environmental Science & Technology*, *35*(9), 1736–1741. <https://doi.org/10.1021/es0002868>
- Bowman, J. J., & Harlock, S. (1998). The Spatial Distribution of Characterised Fly-Ash Particles and Trace Metals in Lake Sediments and Catchment Mosses: Ireland. *Water, Air, and Soil Pollution*, *106*(3), 263–286. <https://doi.org/10.1023/A:1005089212101>
- Boyle, J. F., Mackay, A. W., Rose, N. L., Flower, R. J., & Appleby, P. G. (1998). Sediment heavy metal record in Lake Baikal: Natural and anthropogenic sources. *Journal of Paleolimnology*, *20*(2), 135–150. <https://doi.org/10.1023/A:1008051701416>

- Broman, D., Näf, C., Wik, M., & Renberg, I. (1990). The importance of spheroidal carbonaceous particles (SCPs) for the distribution of particulate polycyclic aromatic hydrocarbons (PAHs) in an estuarine-like urban coastal water area. *Chemosphere*, *21*(1), 69–77. [https://doi.org/10.1016/0045-6535\(90\)90379-8](https://doi.org/10.1016/0045-6535(90)90379-8)
- Butts, C., & Gildersleeve, B. (1948). Geology and Mineral Resources of the Paleozoic Area in Northwest Georgia. *Department of Mines, Mining and Geology, Bulletin No. 54*, 49–52.
- Cameron, N. G., Tyler, P. A., Rose, N. L., Hutchinson, S., & Appleby, P. G. (1993). The recent palaeolimnology of Lake Nicholls, Mount Field National Park, Tasmania. *Hydrobiologia*, *269*(1), 361–370. <https://doi.org/10.1007/BF00028035>
- Comtois, P., Alcazar, P., & Neron, D. (1999). Pollen counts statistics and its relevance to precision. *Aerobiologia*, *15*, 19–28. <https://doi.org/10.1023/A:1007501017470>
- Cowan, E. A., Epperson, E. E., Seramur, K. C., Brachfeld, S. A., & Hageman, S. J. (2017). Magnetic susceptibility as a proxy for coal ash pollution within riverbed sediments in a watershed with complex geology (southeastern USA). *Environmental Earth Sciences*, *76*(19), 657. <https://doi.org/10.1007/s12665-017-6996-8>
- Cowan, E. A., Seramur, K. C., & Hageman, S. J. (2013). Magnetic susceptibility measurements to detect coal fly ash from the Kingston Tennessee spill in Watts Bar Reservoir. *Environmental Pollution*, *174*, 179–188. <https://doi.org/10.1016/j.envpol.2012.11.023>
- Curtis, C. J., Rose, N. L., Khanzada, T., Yang, H., & Humphries, M. (2023). Anthropocene environmental change in an overlooked South African lake: Mountain Lake, Matatiele, Eastern Cape. *Transactions of the Royal Society of South Africa*, *78*(1–2), 45–66. <https://doi.org/10.1080/0035919X.2023.2177361>

- Deonarine, A., Kolker, A., & Doughten, M. (2015). *Trace Elements in Coal Ash* (Fact Sheet 2015-3037). United States Geological Survey (USGS).  
<http://dx.doi.org/10.3133/fs20153037>
- Deonarine, A., Schwartz, G. E., & Ruhl, L. S. (2023). Environmental Impacts of Coal Combustion Residuals: Current Understanding and Future Perspectives. *Environmental Science & Technology*, 57(5), 1855–1869. <https://doi.org/10.1021/acs.est.2c06094>
- Doberstein, C. P., Karr, J. R., & Conquest, L. L. (2000). The effect of fixed-count subsampling on macroinvertebrate biomonitoring in small streams. *Freshwater Biology*, 44(2), 355–371. <https://doi.org/10.1046/j.1365-2427.2000.00575.x>
- Dragović, S., Čujić, M., Slavković-Beškoski, L., Gajić, B., Bajat, B., Kilibarda, M., & Onjia, A. (2013). Trace element distribution in surface soils from a coal burning power production area: A case study from the largest power plant site in Serbia. *CATENA*, 104, 288–296.  
<https://doi.org/10.1016/j.catena.2012.12.004>
- EIA. (2023). *U.S. Energy Information Administration—EIA - Independent Statistics and Analysis* (International Energy Outlook 2023 IEO 2023). U.S. Energy Information Administration.  
<https://www.eia.gov/outlooks/aeo/data/browser/#/?id=7-IEO2023&region=0-0&cases=Reference&start=2020&end=2050&f=A&linechart=~~~~~Reference-d230822.21-7-IEO2023&ctype=linechart&sid=&sourcekey=0>
- EPA. (2022). *Toxics Release Inventory (TRI) Program* [Overviews and Factsheets].  
<https://www.epa.gov/toxics-release-inventory-tri-program>
- EPA. (2023, 18). *EPA Facility Level GHG Emissions Data*.  
<https://ghgdata.epa.gov/ghgp/main.do>

- Fiałkiewicz-Kozieł, B., Łokas, E., Smieja-Król, B., Turner, S., De Vleeschouwer, F., Woszczyk, M., Marcisz, K., Gałka, M., Lamentowicz, M., Kołaczek, P., Hajdas, I., Karpińska-Kołaczek, M., Kołtonik, K., Mróz, T., Roberts, S., Rose, N., Krzykawski, T., Boom, A., & Yang, H. (2023). The Śnieżka peatland as a candidate Global boundary Stratotype Section and Point for the Anthropocene series. *The Anthropocene Review*, *10*(1), 288–315. <https://doi.org/10.1177/20530196221136425>
- Fritsch, D. (2021, December 15). *Of the operating U.S. coal-fired power plants, 28% plan to retire by 2035*. EIA. <https://www.eia.gov/todayinenergy/detail.php?id=50658>
- Garcés-Pastor, S., Fletcher, W. J., & Ryan, P. A. (2023). Ecological impacts of the industrial revolution in a lowland raised peat bog near Manchester, NW England. *Ecology and Evolution*, *13*(2), e9807. <https://doi.org/10.1002/ece3.9807>
- Gopinathan, P., Santosh, M. S., Dileepkumar, V. G., Subramani, T., Reddy, R., Masto, R. E., & Maity, S. (2022). Geochemical, mineralogical and toxicological characteristics of coal fly ash and its environmental impacts. *Chemosphere*, *307*, 135710. <https://doi.org/10.1016/j.chemosphere.2022.135710>
- Han, Y., Zhisheng, A., Lei, D., Zhou, W., Zhang, L., Zhao, X., Yan, D., Arimoto, R., Rose, N. L., Roberts, S. L., Li, L., Tang, Y., Liu, X., Fu, X., Schneider, T., Hou, X., Lan, J., Tan, L., Liu, X., ... Dusek, U. (2023). The Sihailongwan Maar Lake, northeastern China as a candidate Global boundary Stratotype Section and Point for the Anthropocene series. *The Anthropocene Review*, *10*(1), 177–200. <https://doi.org/10.1177/20530196231167019>
- Harkness, J. S., Sulkin, B., & Vengosh, A. (2016). Evidence for Coal Ash Ponds Leaking in the Southeastern United States. *Environmental Science & Technology*, *50*(12), 6583–6592. <https://doi.org/10.1021/acs.est.6b01727>

- Head, M. J., Steffen, W., Fagerlind, D., Waters, C. N., Poirier, C., Syvitski, J., Zalasiewicz, J. A., Barnosky, A. D., Cearreta, A., Jeandel, C., Leinfelder, R., McNeill, J. R., Rose, N. L., Summerhayes, C., Wapre, M., & Zinke, J. (2022). The Great Acceleration is real and provides a quantitative basis for the proposed Anthropocene Series/Epoch. *Episodes*, 45(4), 359–376. <https://doi.org/10.18814/epiiugs/2021/021031>
- Heiri, O., Lotter, A. F., & Lemcke, G. (2001). Loss on ignition as a method for estimating organic and carbonate content in sediments: Reproducibility and comparability of results. *Journal of Paleolimnology*, 25(1), 101–110. <https://doi.org/10.1023/A:1008119611481>
- Herron, C. (2022). *Exploring Geochemical Methods to Measure Arsenic-Dissolved Organic Matter Complexes and Coal Combustion Residuals in Surface Water*. <https://etd.auburn.edu/handle/10415/8426>
- Himson, S., Williams, M., Zalasiewicz, J., Waters, C. N., McGann, M., England, R., Jaffe, B. E., Boom, A., Holmes, R., Sampson, S., Pye, C., Berrio, J. C., Tyrrell, G., Wilkinson, I. P., Rose, N., Gaca, P., & Cundy, A. (2023). The San Francisco Estuary, USA as a reference section for the Anthropocene series. *The Anthropocene Review*, 10(1), 87–115. <https://doi.org/10.1177/20530196221147607>
- Hsu, P. L., & Robbins, H. (1947). Complete Convergence and the Law of Large Numbers. *Proceedings of the National Academy of Sciences*, 33(2), 25–31. <https://doi.org/10.1073/pnas.33.2.25>
- Hsu, W. T., Liu, M. C., Hung, P. C., Chang, S. H., & Chang, M. B. (2016). PAH emissions from coal combustion and waste incineration. *Journal of Hazardous Materials*, 318, 32–40. <https://doi.org/10.1016/j.jhazmat.2016.06.038>

- Inoue, J., Takenaka, N., Okudaira, T., & Kuwae, M. (2022). The record of sedimentary spheroidal carbonaceous particles (SCPs) in Beppu Bay, southern Japan, compared to historical trends of industrial activity and atmospheric pollution: Further evidence for SCPs as a marker for Anthropocene industrialization. *The Anthropocene Review*, *10*(2), 541–555. <https://doi.org/10.1177/20530196221076577>
- Kaiser, J., Abel, S., Arz, H. W., Cundy, A. B., Dellwig, O., Gaca, P., Gerdts, G., Hajdas, I., Labrenz, M., Milton, J. A., Moros, M., Primpke, S., Roberts, S. L., Rose, N. L., Turner, S. D., Voss, M., & Ivar do Sul, J. A. (2023). The East Gotland Basin (Baltic Sea) as a candidate Global boundary Stratotype Section and Point for the Anthropocene series. *The Anthropocene Review*, *10*(1), 25–48. <https://doi.org/10.1177/20530196221132709>
- Kemp, A. C., Wright, A. J., & Cahill, N. (2020). Enough is Enough, or More is More? Testing the Influence of Foraminiferal Count Size on Reconstructions of Paleo-Marsh Elevation. *Journal of Foraminiferal Research*, *50*(3), 266–278. <https://doi.org/10.2113/gsjfr.50.3.266>
- Kinniburgh, D. G., van Riemsdijk, W. H., Koopal, L. K., Borkovec, M., Benedetti, M. F., & Avena, M. J. (1999). Ion binding to natural organic matter: Competition, heterogeneity, stoichiometry and thermodynamic consistency. *Colloids and Surfaces A: Physicochemical and Engineering Aspects*, *151*(1), 147–166. [https://doi.org/10.1016/S0927-7757\(98\)00637-2](https://doi.org/10.1016/S0927-7757(98)00637-2)
- Koinig, K. A., Kamenik, C., Schmidt, R., Agustí-Panareda, A., Appleby, P., Lami, A., Prazakova, M., Rose, N., Schnell, Ø. A., Tessadri, R., Thompson, R., & Psenner, R. (2002). Environmental changes in an alpine lake (Gossenköllesee, Austria) over the last

- two centuries – the influence of air temperature on biological parameters. *Journal of Paleolimnology*, 28(1), 147–160. <https://doi.org/10.1023/A:1020332220870>
- Korhola, A., Sorvari, S., Rautio, M., Appleby, P. G., Dearing, J. A., Hu, Y., Rose, N., Lami, A., & Camerson, N. G. (2002). A multi-proxy analysis of climate impacts on the recent development of subarctic Lake Saanajärvi in Finnish Lapland. *Journal of Paleolimnology*, 28(1), 59–77. <https://doi.org/10.1023/A:1020371902214>
- Külaots, I., Hurt, R. H., & Suuberg, E. M. (2004). Size distribution of unburned carbon in coal fly ash and its implications. *Fuel*, 83(2), 223–230. [https://doi.org/10.1016/S0016-2361\(03\)00255-2](https://doi.org/10.1016/S0016-2361(03)00255-2)
- Landers, D. H., Simonich, S., Jaffe, D., Geiser, L., Campbell, D. H., Schwindt, A., Schreck, C., Kent, M., Hafner, W., Taylor, H. E., Hageman, K., Usenko, S., Schrlau, J., Rose, N., Blett, T., & Erway, M. M. (2008). *The Fate, Transport, and Ecological Impacts of Airborne Contaminants in Western National Parks (USA)* (EPA/600/R-07/138; pp. 1–291). U.S. Environmental Protection Agency, Office of Research and Development, NHEERL, Western Ecology Division.
- Larsen, J. (2000). Recent changes in diatom-inferred pH, heavy metals, and spheroidal carbonaceous particles in lake sediments near an oil refinery at Mongstad, Western Norway. *Journal of Paleolimnology*, 23(4), 343–363. <https://doi.org/10.1023/A:1008196306748>
- Lima, A. L. C., Farrington, J. W., & Reddy, C. M. (2005). Combustion-Derived Polycyclic Aromatic Hydrocarbons in the Environment—A Review. *Environmental Forensics*, 6(2), 109–131. <https://doi.org/10.1080/15275920590952739>

- Ljung, K., Schoon, P. L., Rudolf, M., Charrieau, L. M., Ni, S., & Filipsson, H. L. (2022). Recent Increased Loading of Carbonaceous Pollution from Biomass Burning in the Baltic Sea. *ACS Omega*, 7(39), 35102–35108. <https://doi.org/10.1021/acsomega.2c04009>
- Lu, M., Jones, S., McKinney, M., Wagner, R., Ahmad, S. M., Kandow, A., Donahoe, R., & Lu, Y. (2022). Sources and composition of natural and anthropogenic hydrocarbons in sediments from an impacted estuary. *Science of The Total Environment*.
- McCarthy, F. M., Patterson, R. T., Head, M. J., Riddick, N. L., Cumming, B. F., Hamilton, P. B., Pisaric, M. F., Gushulak, A. C., Leavitt, P. R., Lafond, K. M., Llew-Williams, B., Marshall, M., Heyde, A., Pilkington, P. M., Moraal, J., Boyce, J. I., Nasser, N. A., Walsh, C., Garvie, M., ... McAndrews, J. H. (2023). The varved succession of Crawford Lake, Milton, Ontario, Canada as a candidate Global boundary Stratotype Section and Point for the Anthropocene series. *The Anthropocene Review*, 10(1), 146–176. <https://doi.org/10.1177/20530196221149281>
- Munawer, M. E. (2018). Human health and environmental impacts of coal combustion and post-combustion wastes. *Journal of Sustainable Mining*, 17(2), 87–96. <https://doi.org/10.1016/j.jsm.2017.12.007>
- Muri, G., Wakeham, S. G., & Rose, N. L. (2006). Records of atmospheric delivery of pyrolysis-derived pollutants in recent mountain lake sediments of the Julian Alps (NW Slovenia). *Environmental Pollution*, 139(3), 461–468. <https://doi.org/10.1016/j.envpol.2005.06.002>
- Orndorff, T. (2021). *The Spatiotemporal Variation of Sediment Characteristics and Nutrient Deposition in Two Coosa River Reservoirs*. <https://etd.auburn.edu/handle/10415/7736>
- Pla, S., Monteith, D., Flower, R., & Rose, N. (2009). The recent palaeolimnology of a remote Scottish loch with special reference to the relative impacts of regional warming and

- atmospheric contamination. *Freshwater Biology*, 54(3), 505–523.  
<https://doi.org/10.1111/j.1365-2427.2008.02127.x>
- Querol, X., Juan, R., Lopez-Soler, A., Fernandez-Turiel, L., & Ruiz, C. R. (1995). *Mobility of trace elements from coal and combustion wastes*.
- Querol, X., Parés, J. M., Plana, F., Fernández-Turiel, J. L., & López-Solar, A. (1994). Fly ash content and distribution in lake sediments around a large power station: Inferences from magnetic susceptibility analysis. *Environmental Geochemistry and Health*, 16(1), 9–18.  
<https://doi.org/10.1007/BF00149588>
- Ramsey, A. B., Faiia, A. M., & Szykiewicz, A. (2019). Eight years after the coal ash spill – Fate of trace metals in the contaminated river sediments near Kingston, eastern Tennessee. *Applied Geochemistry*, 104, 158–167.  
<https://doi.org/10.1016/j.apgeochem.2019.03.008>
- Renberg, I., & Wik, M. (1985). Carbonaceous particles in lake sediments. Pollutants from fossil fuel combustion. *Ambio*, 14, 161–163.
- Ribeiro, J., Silva, T. F., Mendonça Filho, J. G., & Flores, D. (2014). Fly ash from coal combustion – An environmental source of organic compounds. *Applied Geochemistry*, 44, 103–110. <https://doi.org/10.1016/j.apgeochem.2013.06.014>
- Rose, N. L. (1990). A method for the extraction of carbonaceous particles from lake sediment. *Journal of Paleolimnology*, 3(1), 45–53. <https://doi.org/10.1007/BF00209299>
- Rose, N. L. (1994). A note on further refinements to a procedure for the extraction of carbonaceous fly-ash particles from sediments. *Journal of Paleolimnology*, 11(2), 201–204. <https://doi.org/10.1007/BF00686866>

- Rose, N. L. (1996). Inorganic fly-ash spheres as pollution tracers. *Environmental Pollution*, 91(2), 245–252. [https://doi.org/10.1016/0269-7491\(95\)00044-5](https://doi.org/10.1016/0269-7491(95)00044-5)
- Rose, N. L. (2008). Quality control in the analysis of lake sediments for spheroidal carbonaceous particles. *Limnology and Oceanography: Methods*, 6(4), 172–179. <https://doi.org/10.4319/lom.2008.6.172>
- Rose, N. L. (2015). Spheroidal Carbonaceous Fly Ash Particles Provide a Globally Synchronous Stratigraphic Marker for the Anthropocene. *Environmental Science & Technology*, 49(7), 4155–4162. <https://doi.org/10.1021/acs.est.5b00543>
- Rose, N. L., & Appleby, P. G. (2005). Regional Applications of Lake Sediment Dating by Spheroidal Carbonaceous Particle Analysis I: United Kingdom. *Journal of Paleolimnology*, 34(3), 349–361. <https://doi.org/10.1007/s10933-005-4925-4>
- Rose, N. L., Appleby, P. G., Boyle, J. F., Mackay, A. W., & Flower, R. J. (1998). The spatial and temporal distribution of fossil-fuel derived pollutants in the sediment record of Lake Baikal, east Siberia. *Journal of Paleolimnology*, 20(2), 151–162. <https://doi.org/10.1023/A:1008064123706>
- Rose, N. L., Harlock, S., & Appleby, P. G. (1999). Within-basin profile variability and cross-correlation of lake sediment cores using the spheroidal carbonaceous particle record. *Journal of Paleolimnology*, 21, 85–96. <https://doi.org/10.1023/A:1008010418680>
- Rose, N. L., Jones, V. J., Noon, P. E., Hodgson, D. A., Flower, R. J., & Appleby, P. G. (2012). Long-Range Transport of Pollutants to the Falkland Islands and Antarctica: Evidence from Lake Sediment Fly Ash Particle Records. *Environmental Science & Technology*, 46(18), 9881–9889. <https://doi.org/10.1021/es3023013>

- Rose, N. L., Milner, A. M., Fitchett, J. M., Langerman, K. E., Yang, H., Turner, S. D., Jourdan, A.-L., Shilland, J., Martins, C. C., de Souza, A. C., & Curtis, C. J. (2020). Natural archives of long-range transported contamination at the remote lake Letšeng-la Letsie, Maloti Mountains, Lesotho. *Science of The Total Environment*, 737, 139642. <https://doi.org/10.1016/j.scitotenv.2020.139642>
- Rose, N. L., & Rippey, B. (2002). The historical record of PAH, PCB, trace metal and fly-ash particle deposition at a remote lake in north-west Scotland. *Environmental Pollution*, 117(1), 121–132. [https://doi.org/10.1016/S0269-7491\(01\)00149-X](https://doi.org/10.1016/S0269-7491(01)00149-X)
- Rose, N. L., Rose, C. L., Boyle, J. F., & Appleby, P. G. (2004). Lake-Sediment Evidence for Local and Remote Sources of Atmospherically Deposited Pollutants on Svalbard. *Journal of Paleolimnology*, 31(4), 499–513. <https://doi.org/10.1023/B:JOPL.0000022548.97476.39>
- Ruhl, L., Vengosh, A., Dwyer, G. S., Hsu-Kim, H., & Deonarine, A. (2010). Environmental Impacts of the Coal Ash Spill in Kingston, Tennessee: An 18-Month Survey. *Environmental Science & Technology*, 44(24), 9272–9278. <https://doi.org/10.1021/es1026739>
- Ruhl, L., Vengosh, A., Dwyer, G. S., Hsu-Kim, H., Deonarine, A., Bergin, M., & Kravchenko, J. (2009). Survey of the Potential Environmental and Health Impacts in the Immediate Aftermath of the Coal Ash Spill in Kingston, Tennessee. *Environmental Science & Technology*, 43(16), 6326–6333. <https://doi.org/10.1021/es900714p>
- Ruhl, L., Vengosh, A., Dwyer, G. S., Hsu-Kim, H., Schwartz, G., Romanski, A., & Smith, S. D. (2012). The Impact of Coal Combustion Residue Effluent on Water Resources: A North

- Carolina Example. *Environmental Science & Technology*, 46(21), 12226–12233.  
<https://doi.org/10.1021/es303263x>
- Schlachter, K. J., & Horn, S. P. (2010). Sample preparation methods and replicability in macroscopic charcoal analysis. *Journal of Paleolimnology*, 44(2), 701–708.  
<https://doi.org/10.1007/s10933-009-9305-z>
- Schneider, L., Rose, N. L., Lintern, A., Sinclair, D., Zawadzki, A., Holley, C., Aquino-López, M. A., & Haberle, S. (2020). Assessing environmental contamination from metal emission and relevant regulations in major areas of coal mining and electricity generation in Australia. *Science of The Total Environment*, 728, 137398.  
<https://doi.org/10.1016/j.scitotenv.2020.137398>
- Schneider, L., Rose, N. L., Myllyvirta, L., Haberle, S., Lintern, A., Yuan, J., Sinclair, D., Holley, C., Zawadzki, A., & Sun, R. (2021). Mercury atmospheric emission, deposition and isotopic fingerprinting from major coal-fired power plants in Australia: Insights from palaeo-environmental analysis from sediment cores. *Environmental Pollution*, 287, 117596. <https://doi.org/10.1016/j.envpol.2021.117596>
- Solovieva, N., Jones, V. J., Nazarova, L., Brooks, S. J., Birks, H. J. B., Grytnes, J.-A., Appleby, P. G., Kauppila, T., Kondratenok, B., Renberg, I., & Ponomarev, V. (2005). Palaeolimnological evidence for recent climatic change in lakes from the northern Urals, arctic Russia. *Journal of Paleolimnology*, 33(4), 463–482.  
<https://doi.org/10.1007/s10933-005-0811-3>
- Steffen, W., Broadgate, W., Deutsch, L., Gaffney, O., & Ludwig, C. (2015). The trajectory of the Anthropocene: The Great Acceleration. *The Anthropocene Review*, 2(1), 81–98.  
<https://doi.org/10.1177/2053019614564785>

- Steffen, W., Crutzen, P. J., & McNeill, J. R. (2007). Are Humans Now Overwhelming the Great Forces of Nature? *Ambio*, *36*(8), 614–621.
- Stegner, M. A., Hadly, E. A., Barnosky, A. D., La Selle, S., Sherrod, B., Anderson, R. S., Redondo, S. A., Viteri, M. C., Weaver, K. L., Cundy, A. B., Gaca, P., Rose, N. L., Yang, H., Roberts, S. L., Hajdas, I., Black, B. A., & Spanbauer, T. L. (2023). The Searsville Lake Site (California, USA) as a candidate Global boundary Stratotype Section and Point for the Anthropocene series. *The Anthropocene Review*, *10*(1), 116–145.  
<https://doi.org/10.1177/20530196221144098>
- Stout, S. A., & Wasielewski, T. N. (2004). Historical and Chemical Assessment of the Sources of PAHs in Soils at a Former Coal-Burning Power Plant, New Haven, Connecticut. *Environmental Forensics*, *5*(4), 195–211. <https://doi.org/10.1080/15275920490886789>
- Stringer, C., Kirby, J. R., & Wilkinson, D. M. (2014). Combining Palaeoecological and Historical Approaches to Investigating Post-Medieval Land Use Change at Sandford Mire, Cumbria, North West England, UK. *Journal of Wetland Archaeology*, *14*(1), 74–90. <https://doi.org/10.1179/1473297114Z.00000000011>
- Swindles, G. T. (2010). Dating recent peat profiles using spheroidal carbonaceous particles (SCPs). *Mires and Peat*, *7*, Article 3.
- Swindles, G. T., Watson, E., Turner, T. E., Galloway, J. M., Hadlari, T., Wheeler, J., & Bacon, K. L. (2015). Spheroidal carbonaceous particles are a defining stratigraphic marker for the Anthropocene. *Scientific Reports*, *5*(1), Article 1. <https://doi.org/10.1038/srep10264>
- Thies, H., Tolotti, M., Nickus, U., Lami, A., Musazzi, S., Guilizzoni, P., Rose, N. L., & Yang, H. (2011). Interactions of temperature and nutrient changes: Effects on phytoplankton in the

- Piburger See (Tyrol, Austria). *Freshwater Biology*, 57(10), 2057–2075.  
<https://doi.org/10.1111/j.1365-2427.2011.02661.x>
- Thomas, E. R., Tetzner, D. R., Roberts, S. L., Turner, S. D., & Rose, N. L. (2023). First evidence of industrial fly-ash in an Antarctic ice core. *Scientific Reports*, 13(1), Article 1.  
<https://doi.org/10.1038/s41598-023-33849-x>
- Thomas, E. R., Vladimirova, D. O., Tetzner, D. R., Emanuelsson, D. B., Humby, J., Turner, S. D., Rose, N. L., Roberts, S. L., Gaca, P., & Cundy, A. B. (2023). The Palmer ice core as a candidate Global boundary Stratotype Section and Point for the Anthropocene series. *The Anthropocene Review*, 10(1), 251–268. <https://doi.org/10.1177/20530196231155191>
- Tiwari, M., Sahu, S. K., Bhangare, R. C., Ajmal, P. Y., & Pandit, G. G. (2014). Elemental characterization of coal, fly ash, and bottom ash using an energy dispersive X-ray fluorescence technique. *Applied Radiation and Isotopes*, 90, 53–57.  
<https://doi.org/10.1016/j.apradiso.2014.03.002>
- Tripp, B. W., Farrington, J. W., & Teal, J. M. (1981). Unburned coal as a source of hydrocarbons in surface sediments. *Marine Pollution Bulletin*, 12(4), 122–126.  
[https://doi.org/10.1016/0025-326X\(81\)90440-9](https://doi.org/10.1016/0025-326X(81)90440-9)
- US EPA. (2014). *Coal Combustion Residuals Impoundment Assessment Reports*.  
<https://www3.epa.gov/epawaste/coal/html/index-4.html>
- US EPA. (2023, June 14). *Coal Ash Basics* [Overviews and Factsheets].  
<https://www.epa.gov/coalash/coal-ash-basics>
- Vachula, R. S., Chipman, M. L., & Hu, F. S. (2017). Holocene climatic change in the Alaskan Arctic as inferred from oxygen-isotope and lake-sediment analyses at Wahoo Lake. *The Holocene*, 27(11), 1631–1644. <https://doi.org/10.1177/0959683617702230>

- Vachula, R. S., Ojeda, A. S., Henderson, E. D., & Inoue, J. (2023). The DiSCPersal model: A simple model for the small-scale atmospheric transport of spheroidal carbonaceous particles (SCPs). *Chemosphere*, 328, 138547.  
<https://doi.org/10.1016/j.chemosphere.2023.138547>
- Vassilev, S. V., & Vassileva, C. G. (1996). Mineralogy of combustion wastes from coal-fired power stations. *Fuel Processing Technology*, 47(3), 261–280.  
[https://doi.org/10.1016/0378-3820\(96\)01016-8](https://doi.org/10.1016/0378-3820(96)01016-8)
- Vengosh, A., Cowan, E. A., Coyte, R. M., Kondash, A. J., Wang, Z., Brandt, J. E., & Dwyer, G. S. (2019). Evidence for unmonitored coal ash spills in Sutton Lake, North Carolina: Implications for contamination of lake ecosystems. *Science of The Total Environment*, 686, 1090–1103. <https://doi.org/10.1016/j.scitotenv.2019.05.188>
- Vengosh, A., Hsu-Kim, H., Ruhl, L., Dwyer, G., Schwartz, G., Romanksi, A., & Smith, D. (2012). *THE IMPACT OF COAL COMBUSTION RESIDUALS ON THE QUALITY OF WATER RESOURCES IN NORTH CAROLINA* (WRI Project No. 11-08-W 414). Water Resources Research Institute of the University of North Carolina.
- Wang, Z., Cowan, E. A., Seramur, K. C., Dwyer, G. S., Wilson, J. C., Karcher, R., Brachfeld, S., & Vengosh, A. (2022). Legacy of Coal Combustion: Widespread Contamination of Lake Sediments and Implications for Chronic Risks to Aquatic Ecosystems. *Environmental Science & Technology*, 56(20), 14723–14733. <https://doi.org/10.1021/acs.est.2c04717>
- Waters, C. N., Turner, S. D., Zalasiewicz, J., & Head, M. J. (2023). Candidate sites and other reference sections for the Global boundary Stratotype Section and Point of the Anthropocene series. *The Anthropocene Review*, 10(1), 3–24.  
<https://doi.org/10.1177/20530196221136422>

- Waters, C. N., Zalasiewicz, J., Summerhayes, C., Barnosky, A. D., Poirier, C., Gałuszka, A., Cearreta, A., Edgeworth, M., Ellis, E. C., Ellis, M., Jeandel, C., Leinfelder, R., McNeill, J. R., Richter, D. deB., Steffen, W., Syvitski, J., Vidas, D., Wagreich, M., Williams, M., ... Wolfe, A. P. (2016). The Anthropocene is functionally and stratigraphically distinct from the Holocene. *Science*, *351*(6269), aad2622.  
<https://doi.org/10.1126/science.aad2622>
- Wik, M., & Renberg, I. (1996). *Environmental records of carbonaceous fly-ash particles from fossil-fuel combustion*. *15*, 193–206. <https://doi.org/10.1007/BF00213040>
- Wu, G., Yang, C., Guo, L., & Wang, Z. (2013). Cadmium contamination in Tianjin agricultural soils and sediments: Relative importance of atmospheric deposition from coal combustion. *Environmental Geochemistry and Health*, *35*(3), 405–416.  
<https://doi.org/10.1007/s10653-012-9503-x>
- Yang, H., Rose, N. L., Boyle, J. F., & Battarbee, R. W. (2001). Storage and distribution of trace metals and spheroidal carbonaceous particles (SCPs) from atmospheric deposition in the catchment peats of Lochnagar, Scotland. *Environmental Pollution*, *115*(2), 231–238.  
[https://doi.org/10.1016/S0269-7491\(01\)00107-5](https://doi.org/10.1016/S0269-7491(01)00107-5)
- Zielinski, R. A., Foster, A. L., Meeker, G. P., & Brownfield, I. K. (2007). Mode of occurrence of arsenic in feed coal and its derivative fly ash, Black Warrior Basin, Alabama. *Fuel*, *86*(4), 560–572. <https://doi.org/10.1016/j.fuel.2006.07.033>

## **Appendix 1: Chapter 2 Supplementary information**

**Table S.2.1.** Site information for Figure 2.5.

Num	Site name	Lat	Long	Ref	Category
1	PJ#1	47.95	-123.42	1	Moderate
2	Golden Lake	46.887	-121.887	1	Moderate
3	Emerald Lake	36.58	-118.67	1	Moderate
4	Snyder	48.62	-113.79	1	Moderate
5	Taylor Lake	40.787	-110.091	2	Moderate
6	Mills Lake	40.29	-105.64	1	Moderate
7	Yaal Chac	20.4	-89.4	2	High
8	Queer Lake	43.8	-74.8	3	Very High
9	Deep Lake	43.617	-74.667	3	Very High
10	Laguna Chica de San Pedro	-36.85	-73.083	4	High
11	Adam Tarn	-51.561	-60.076	5	Low
12	Nunatak Lake	67.952	-49.81	6	Low
13	Sombre Lake	-60.717	-45.6	5	Low
14	Apavatn	64.3	-20.667	2	Low
15	Lough Veagh	55.042	-7.967	7	High
16	Loch Teanga	57.324	-7.289	8	Moderate
17	Lough Brantry	54.425	-6.85	9	High
18	Merja Bokka	34.367	-6.283	10	High
19	Merja Zerga	34.833	-6.283	10	High

20	Lough Mourne	54.767	-5.8	9	Very High
21	Loch Shiel	56.836	-5.5	9	High
22	Loch Coire Fionnaraich	56.836	-5.5	11	Moderate
23	Laguna Cimera	40.267	-5.305	12	High
24	Laguna Grande de Gredos	57.236	-4.553	13	High
25	Loch Ness	53.015	-4.015	14	High
26	Llyn Llagi	54.482	-3.299	7	High
27	Pinkworthy Pond	56.933	-3.168	9	Very High
28	Scoat Tarn	54.482	-3.299	9	Very High
29	Loch Muick	56.933	-3.168	9	High
30	Agden Reservoir	53.429	-1.61	9	Very High
31	Groby Pool	52.663	-1.301	15	Very High
32	Estany Redo	42.643	0.77	16	High
33	Barnby Broad	52.157	1.649	17	High
34	Svartatjönn	60.883	5.167	18	Moderate
35	Lac Noir	45.417	7.117	12	Moderate
36	Hagelsee	46.667	8.033	19	High
37	Øvre Neådalsvatn	62.775	9	12	Moderate

38	Merja Chetane	37.15	9.1	10	High
39	Jorisee	46.783	9.967	2	High
40	Lange Sø	55.517	10.25	20	Very High
41	Lake Garda	45.583	10.621	21	Very High
42	Arresjøen	79.675	10.853	12	Low
43	Piburgersee	45.192	10.883	22	Moderate
44	Gossenköllesee	47.217	11.017	23	Moderate
45	Lago di Latte	46.726	11.073	12	High
46	Lago di Canzolino	46.083	11.226	21	Very High
47	Birgervatnet	79.81	11.629	24	Moderate
48	Buvatten	57.917	12.1	25	High
49	Jezero Ledvica	46.34	13.787	26	Moderate
50	Neusiedler	47.833	16.75	21	Very High
51	Nizne Terianske Pleso	49.167	20	12	High
52	Ladove	49.184	20.163	2	High
53	Granastjärn	64.617	20.167	25	Moderate
54	Saanajarvi	69.083	20.867	27	Moderate
55	Lacul Negru	45.359	22.829	28	High
56	Uluabat	40.19	28.542	2	High

57	Lake Qarun	30.6	29.483	29	High
58	Lake Edku	31.267	31.217	10	High
59	Potri	59.233	37.542	30	Very High
60	Dlugi Staw Gasiencowy	49.228	37.678	12	High
61	Zielowny Staw Gasiencowy	49.225	37.692	12	High
62	Zibakenar Lagoon, Caspian Sea	37.503	49.886	31	High
63	Mitrofanovskoe	67.85	58.983	32	Moderate
64	Vanuk-ty	68	62.75	32	Moderate
65	Kvadratnoye	51.367	105.183	2	Moderate
66	Lake Baikal	52.45	106.133	33	Moderate
67	Donghu	30.55	114.4	34	Very High
68	Tai Hu	31.332	120.08	35	Very High
69	Xiaolongwan	42.3	126.36	36	High
70	Akagi-konuma	36.532	139.192	37	Very High
71	Lake Nicholls	-42.42	146.7	38	Low
72	Laguna El Ocho	-34.033	-70.317	39	Very High

73	Laguna Negra	-38.633	-70.133	39	Very High
74	Huzenbacher See	48.574	8.348	40	Very High
75	Longgan Lake	29.867	115.917	41	Very High
76	Sawanoike Pond	35.05	135.7	42	Very High
77	San Fransico Estuary	37.5495	122.1831	43	Very High
78	Searsville Lake	37.4068	122.2377	44	Very High
79	Palmer Ice Core	73.8521	65.4526	45	Very High
80	Crawford Lake	43.4686	79.9487	46	Very High
81	Sniezka, Sudetes	50.7391	15.7077	47	Very High
82	East Gotland Basin	57.283	20.1204	48	Low
83	Sihailongwan Maar	42.2868	126.6012	49	Very High
84	Beppu Bay	33.2778	131.5373	50	Very High

85	Letšeng-la Letsie	-30.311	28.16647	51	High
86	Mountain Lake	-30.4009	28.81728	52	Very High
87	Lake Glenbawn	-32.094	150.9891	53	High
88	Traralgon Railway Reservoir	-38.2098	146.5298	53	Very High
89	Hasse Lake	53.48722	114.1731	54	Very High

### References for Table S1

- (1) Landers, D.H.; Simonich, S.M., Jaffe, D.A.; Geiser, L.; Campbell, D.H.; Schwindt, A.; Schreck, C.; Kent, M.; Hafner, W.; Taylor, H.E.; Hageman, K. J.; Usenko, S.; Ackerman, L.; Schrlau, J.; Rose, N. L.; Blett, T.; Erway, M. M. *The fate, transport and ecological impacts of airborne contaminants in western National Parks (USA)*. EPA/600/R-07/138, 1-291. Corvallis, OR, U.S. Environmental Protection Agency, Office of Research and Development, NHEERL, Western Ecology Division, **2008**.
- (2) Rose, N.L. unpublished data from Rose, N. L. Spheroidal Carbonaceous Fly Ash Particles Provide a Globally Synchronous Stratigraphic Marker for the Anthropocene. *Environ. Sci. Technol.* **2015**, 49 (7), 4155–4162. <https://doi.org/10.1021/acs.est.5b00543>.
- (3) Charles, D. F.; Binford, M. W.; Furlong, E. T.; Hites, R. A.; Mitchell, M. J.; Norton, S. A.; Oldfield, F.; Paterson, M. J.; Smol, J. P.; Uutala, A. J.; White, J. R.; Whitehead, D. R.; Wise,

R. J. Palaeoecological investigation of recent lake acidification in the Adirondack Mountains, N.Y. *J. Paleolimnol.* **1990**, *3*, 195-241.

(4) Chirinos, L.; Rose, N. L.; Urrutia, R.; Muñoz, P.; Torrejón, F.; Torres, L.; Cruces, F.; Araneda, A.; Zaror, C. Environmental evidence of fossil fuel pollution in Laguna Chica de San Pedro lake sediments (Central Chile). *Environmental Pollution.* **2006**, *141*, 247-256.

(5) Rose, N. L.; Jones, V. J.; Noon, P. E.; Hodgson, D. A.; Flower, R. J.; Appleby, P. G. Long-range transport of pollutants to the Falkland Islands and Antarctica: Evidence from lake sediment fly-ash particle records. *Environ. Sci. Technol.* **2012**, *46* 9881-9889.

(6) Bindler, R.; Renberg, I.; Appleby, P. G.; Anderson, N. J.; Rose, N. L. Mercury accumulation rates and spatial patterns in lake sediments from west Greenland: A coast to ice margin transect. *Environ. Sci. Technol.* **2001**, *35* (9), 1736-1741.

(7) Rose, N. L.; Harlock, S.; Appleby, P. G.; Battarbee, R. W. Dating of recent lake sediments in the United Kingdom and Ireland using spheroidal carbonaceous particle (SCP) concentration profiles. *Holocene* **1995**, *5* 328-335.

(8) Rose, N. L. Inorganic ash spheres as pollution tracers. *Environ. Pollut.* **1996**, *91* 245-252.

(9) Rose, N. L.; Appleby, P. G. Regional applications of lake sediment dating by spheroidal carbonaceous particle analysis I. United Kingdom. *J. Paleolimnol.* **2005**, *34* 349-361.

(10) Rose, N. L.; Flower, R. J.; Appleby, P. G. Spheroidal carbonaceous particles (SCPs) as indicators of atmospherically deposited pollutants in North African wetlands of conservation importance. *Atmos. Environ.* **2003**, *37* 1655-1663.

(11) Pla, S.; Monteith, D.; Flower, R. J.; Rose, N.L. The recent palaeolimnology of a remote Scottish loch with special reference to the relative impacts of regional warming and atmospheric contamination. *Freshwat. Biol.* **2009**, *54* 505-523.

(12) Rose, N. L.; Harlock, S.; Appleby, P. G. The spatial and temporal distributions of spheroidal carbonaceous fly-ash particles (SCP) in the sediment records of European mountain lakes. *Wat. Air Soil Pollut.* **1999**, *113* (1-4), 1-32.

(13) Toro, M.; Flower, R. J.; Rose, N.; Stevenson, A. C. The sedimentary record of the recent history in a high mountain lake in central Spain. *Verh. Internat. Verein. Limnol.* **1993**, *25* 1108-1112.

(14) Jones, V. J.; Battarbee, R. W.; Rose, N. L.; Curtis, C.; Appleby, P. G.; Harriman, R.; Shine, A. J. Evidence for the pollution of Loch Ness from the analysis of its recent sediments. *Sci. Tot. Environ.* **1997**, *203* (1), 37-49.

(15) Davidson, T. A.; Sayer, C. D.; Bennion, H.; David, C.; Rose, N. L.; Wade, M. P.. A 250 year comparison of historical, macrofossil and pollen records of aquatic plants in a shallow

lake. *Freshwat. Biol.* **2005**, *50* 1671-1686.

(16) Rose, N. L.; Yang, H.; Fernández, P.; Grimalt, J.O. Trace metals, fly-ash particles and persistent organic pollutants in European remote mountain lakes. In: Huber, U.M.; Bugmann, H.K.M.; Reasoner, M.A. Eds.; *Global change and mountain regions: An overview of current knowledge*. Springer, Dordrecht. **2005** pp. 123-132.

(17) Bennion, H.; Burgess, A.; Boyle, J.; Appleby, P.G.; Rose, N.L.; Sayer, C.; Theophile, S. *Sediment survey of the Suffolk Broads*. Final report to English Nature (NB/T/806/02-04). Environmental Change Research Centre, University College London Research Report No. 92. **2003**.

(18) Larsen, J. Recent changes in diatom-inferred pH, heavy metals, and spheroidal carbonaceous particles in lake sediments near an oil refinery at Mongstad, western Norway. *J. Paleolimnol.* **2000**, *23*, 343-363.

(19) Lotter, A. F.; Appleby, P. G.; Bindler, R.; Dearing, J. A.; Grytnes, J.-A.; Hofmann, W.; Kamenik, C.; Lami, A.; Livingstone, D. M.; Ohlendorf, C.; Rose, N.; Sturm, M. The sediment record of the past 200 years in a Swiss high-alpine lake: Hagelseewli (2339 m a.s.l.). *J. Paleolimnol.* **2002**, *28*, 111-127.

(20) Odgaard, B. V. The sedimentary record of spheroidal carbonaceous fly-ash particles in shallow Danish lakes. *J. Paleolimnol.* **1993**, *8*, 171-187.

- (21) Tolotti, M. *et al.* unpublished data from Rose, N. L. Spheroidal Carbonaceous Fly Ash Particles Provide a Globally Synchronous Stratigraphic Marker for the Anthropocene. *Environ. Sci. Technol.* **2015**, 49 (7), 4155–4162. <https://doi.org/10.1021/acs.est.5b00543>.
- (22) Thies, H.; Tolotti, M.; Nickus, U.; Lami, A.; Musazzi, S.; Guilizzoni, P.; Rose, N. L.; Yang, H. Interactions of temperature and nutrient changes: effects on phytoplankton in the Piburger See (Tyrol, Austria). *Freshwat. Biol.* **2012**, 57 2057-2075.
- (23) Koinig, K. A.; Kamenik, C.; Schmidt, R.; Agusti-Panareda, A.; Appleby, P. G.; Lami, A.; Prazakova, M.; Rose, N. L.; Schnell, Ø. A.; Tessadri, R.; Thompson, R.; Psenner, R. Environmental changes in an alpine lake (Gossenköllesee, Austria) over the last two centuries - the influence of air temperature on biological parameters. *J. Paleolimnol.* **2002**, 28 147-160.
- (24) Rose, N. L.; Rose, C. L.; Boyle, J. F.; Appleby, P. G. Lake sediment evidence for local and remote sources of atmospherically deposited pollutants on Svalbard. *J. Paleolimnol.* **2004**, 31 499-513.
- (25) Renberg, I. ; Wik, M. Carbonaceous particles in lake sediments. Pollutants from fossil fuel combustion. *Ambio* **1985**, 14, 161-163.
- (26) Muri, G.; Wakeham, S.; Rose, N. L. Records of atmospheric delivery of pyrolysis-derived pollutants in recent mountain lake sediments of the Julian Alps (NW Slovenia).

*Environ. Pollut.* **2006**, 139 461-468.

(27) Korhola, A.; Sorvari, S.; Rautio, M.; Appleby, P. G.; Dearing, J. A.; Hu, Y.; Rose, N.; Lami, A.; Cameron, N. G. A multi-proxy analysis of climate impacts on the recent development of subarctic Lake Saanajarvi in Finnish Lapland. *J. Paleolimnol.* **2002**, 28 (1), 59-77.

(28) Rose, N. L.; Cogalniceanu, D.; Appleby, P. G.; Brancelj, A.; Camarero, L.; Fernández, P.; Grimalt, J. O.; Kernan, M.; Lami, A.; Musazzi, S.; Quiroz, R.; Velle, G. Atmospheric contamination and ecological changes inferred from the sediment record of Lacul Negru in the Retezat National Park, Romania. *Adv. Limnol.* **2009**, 62 319-350.

(29) Flower, R. J.; Stickley, C.; Rose, N. L.; Peglar, S. M.; Fathi, A. A.; Appleby, P. G. Environmental changes at the desert margin: an assessment of recent paleolimnological records in Lake Qarun, Middle Egypt. *J. Paleolimnol.* **2006**, 35, 1-24.

(30) Punning, J. M.; Liblik, V.; Alliksaar, T. History of fly ash emission and palaeorecords of atmospheric deposition in the oil shale combustion area. *Oil Shale* **1997**, 14 (3), 347-362.

(31) Haghani, S. *et al.* unpublished data from Rose, N. L. Spheroidal Carbonaceous Fly Ash Particles Provide a Globally Synchronous Stratigraphic Marker for the Anthropocene. *Environ. Sci. Technol.* **2015**, 49 (7), 4155–4162. <https://doi.org/10.1021/acs.est.5b00543>.

- (32) Solovieva, N.; Jones, V. J.; Nazarova, L.; Brooks, S. J.; Birks, H. J. B.; Grytnes, J.-A.; Appleby, P. G.; Kauppila, T.; Kondratenok, B. M.; Renberg, I.; Ponomarev, V.. Palaeolimnological evidence for recent climatic change in lakes from the northern Urals, arctic Russia. *J. Paleolimnol.* **2005**, *33* 463-482.
- (33) Rose, N. L.; Appleby, P. G.; Boyle, J. F.; Mackay, A. W.; Flower, R. J. The spatial and temporal distribution of fossil-fuel derived pollutants in the sediment record of Lake Baikal, eastern Siberia. *J. Paleolimnol.* **1998**, *20* (2), 151-162.
- (34) Boyle, J. F.; Rose, N. L.; Bennion, H.; Yang, H.; Appleby, P. G. Environmental impacts in the Jiangnan plain: Evidence from lake sediments. *Wat. Air Soil Pollut.* **1999**, *112* (1-2), 21-40.
- (35) Rose, N. L.; Boyle, J. F.; Du, Y.; Yi, C.; Dai, X.; Appleby, P. G.; Bennion, H.; Cai, S.; Yu, L. Sedimentary evidence for changes in the pollution status of Taihu in the Jiangsu region of eastern China. *J. Paleolimnol.* **2004**, *32* 41-51.
- (36) Panizzo, V. N.; Mackay, A. W.; Rose, N. L.; Rioual, P.; Leng, M. J. Recent palaeolimnological change recorded in Lake Xiaolongwan, northeast China: Climatic versus anthropogenic forcing. *Quat. Internat.* **2013**, *290-291* 322-334.
- (37) Nagafuchi, O.; Rose, N. L.; Hoshika, A.; Satake, K. The temporal record and sources of atmospherically deposited fly-ash particles in Lake Akagi-konuma, a Japanese mountain lake.

*J. Paleolimnol.* **2009**, 42 359-371.

(38) Cameron, N. G.; Tyler, P. A.; Rose, N. L.; Hutchinson, S.; Appleby, P. G. The recent palaeolimnology of Lake Nicholls, Mount Field National Park, Tasmania. *Hydrobiol.* **1993**, 269/270 361-370.

(39) von Gunten, H. R.; Sturm, M.; Moser, R. N. Age modelling of young non-varved lake sediments: methods and limits. Examples from two lakes in central Chile. *J. Paleolimnol.* **1997**, 31 (8), 2193-2197.

(40) Hilgers, E.; Thies, H.; Kalbfus, W. A <sup>210</sup>Pb dated sediment record on heavy metals, polycyclic aromatic hydrocarbons and soot spherules for a dystrophic mountain lake. *Verh. Internat. Verein. Limnol.* **1993**, 25 1091-1094.

(41) Wu, Y.; Wang, S.; Xia, W.; Liu, J. Dating recent lake sediments using spheroidal carbonaceous particle (SCP). *Chinese Sci. Bull.* **2005**, 50 (10), 1016-1020.

(42) Yoshikawa, S.; Yamaguchi, S.; Hata, A. Paleolimnological investigation of recent acidity changes in Sawanoike Pond, Kyoto, Japan. *J. Paleolimnol.* **2000**, 23 (3), 285-304.

(43) Himson, S.; Williams, M.; Zalasiewicz, J.; Waters, C. N.; McGann, M.; England, R.; Jaffe, B. E.; Boom, A.; Holmes, R.; Sampson, S.; Pye, C.; Berrio, J. C.; Tyrrell, G.; Wilkinson, I. P.; Rose, N.; Gaca, P.; Cundy, A. The San Francisco Estuary, USA as a Reference Section for the

Anthropocene Series. *The Anthropocene Review* **2023**, 10 (1), 87–115.

<https://doi.org/10.1177/20530196221147607>.

(44) Stegner, M. A.; Hadly, E. A.; Barnosky, A. D.; La Selle, S.; Sherrod, B.; Anderson, R. S.; Redondo, S. A.; Viteri, M. C.; Weaver, K. L.; Cundy, A. B.; Gaca, P.; Rose, N. L.; Yang, H.; Roberts, S. L.; Hajdas, I.; Black, B. A.; Spanbauer, T. L. The Searsville Lake Site (California, USA) as a Candidate Global Boundary Stratotype Section and Point for the Anthropocene Series. *The Anthropocene Review* **2023**, 10 (1), 116–145. <https://doi.org/10.1177/20530196221144098>.

(45) Thomas, E. R.; Vladimirova, D. O.; Tetzner, D. R.; Emanuelsson, D. B.; Humby, J.; Turner, S. D.; Rose, N. L.; Roberts, S. L.; Gaca, P.; Cundy, A. B. The Palmer Ice Core as a Candidate Global Boundary Stratotype Section and Point for the Anthropocene Series. *The Anthropocene Review* **2023**, 10 (1), 251–268. <https://doi.org/10.1177/20530196231155191>.

(46) McCarthy, F. M.; Patterson, R. T.; Head, M. J.; Riddick, N. L.; Cumming, B. F.; Hamilton, P. B.; Pisaric, M. F.; Gushulak, A. C.; Leavitt, P. R.; Lafond, K. M.; Llew-Williams, B.; Marshall, M.; Heyde, A.; Pilkington, P. M.; Moraal, J.; Boyce, J. I.; Nasser, N. A.; Walsh, C.; Garvie, M.; Roberts, S.; Rose, N. L.; Cundy, A. B.; Gaca, P.; Milton, A.; Hajdas, I.; Crann, C. A.; Boom, A.; Finkelstein, S. A.; McAndrews, J. H. The Varved Succession of Crawford Lake, Milton, Ontario, Canada as a Candidate Global Boundary Stratotype Section and Point for the Anthropocene Series. *The Anthropocene Review* **2023**, 10 (1), 146–176. <https://doi.org/10.1177/20530196221149281>.

(47) Fiałkiewicz-Kozieł, B.; Łokas, E.; Smieja-Król, B.; Turner, S.; De Vleeschouwer, F.; Woszczyk, M.; Marcisz, K.; Gałka, M.; Lamentowicz, M.; Kołaczek, P.; Hajdas, I.; Karpińska-Kołaczek, M.; Kołtonik, K.; Mróz, T.; Roberts, S.; Rose, N.; Krzykawski, T.; Boom, A.; Yang, H. The Śnieżka Peatland as a Candidate Global Boundary Stratotype Section and Point for the Anthropocene Series. *The Anthropocene Review* **2023**, 10 (1), 288–315.  
<https://doi.org/10.1177/20530196221136425>.

(48) Kaiser, J.; Abel, S.; Arz, H. W.; Cundy, A. B.; Dellwig, O.; Gaca, P.; Gerdts, G.; Hajdas, I.; Labrenz, M.; Milton, J. A.; Moros, M.; Primpke, S.; Roberts, S. L.; Rose, N. L.; Turner, S. D.; Voss, M.; Ivar do Sul, J. A. The East Gotland Basin (Baltic Sea) as a Candidate Global Boundary Stratotype Section and Point for the Anthropocene Series. *The Anthropocene Review* **2023**, 10 (1), 25–48. <https://doi.org/10.1177/20530196221132709>.

(49) Han, Y.; Zhisheng, A.; Lei, D.; Zhou, W.; Zhang, L.; Zhao, X.; Yan, D.; Arimoto, R.; Rose, N. L.; Roberts, S. L.; Li, L.; Tang, Y.; Liu, X.; Fu, X.; Schneider, T.; Hou, X.; Lan, J.; Tan, L.; Liu, X.; Hu, J.; Cao, Y.; Liu, W.; Wu, F.; Wang, T.; Qiang, X.; Chen, N.; Cheng, P.; Hao, Y.; Wang, Q.; Chu, G.; Guo, M.; Han, M.; Tan, Z.; Wei, C.; Dusek, U. The Sihailongwan Maar Lake, Northeastern China as a Candidate Global Boundary Stratotype Section and Point for the Anthropocene Series. *The Anthropocene Review* **2023**, 10 (1), 177–200.  
<https://doi.org/10.1177/20530196231167019>.

(50) Inoue, J.; Takenaka, N.; Okudaira, T.; Kuwae, M. The Record of Sedimentary Spheroidal Carbonaceous Particles (SCPs) in Beppu Bay, Southern Japan, Compared to Historical Trends of

Industrial Activity and Atmospheric Pollution: Further Evidence for SCPs as a Marker for Anthropocene Industrialization. *The Anthropocene Review* **2022**, 20530196221076577.

<https://doi.org/10.1177/20530196221076577>.

(51) Rose, N. L.; Milner, A. M.; Fitchett, J. M.; Langerman, K. E.; Yang, H.; Turner, S. D.; Jourdan, A.-L.; Shilland, J.; Martins, C. C.; de Souza, A. C.; Curtis, C. J. Natural Archives of Long-Range Transported Contamination at the Remote Lake Letšeng-La Letsie, Maloti Mountains, Lesotho. *Science of The Total Environment* **2020**, 737, 139642.

<https://doi.org/10.1016/j.scitotenv.2020.139642>.

(52) Curtis, C. J.; Rose, N. L.; Khanzada, T.; Yang, H.; Humphries, M. Anthropocene Environmental Change in an Overlooked South African Lake: Mountain Lake, Matatiele, Eastern Cape. *Transactions of the Royal Society of South Africa* **2023**, 78 (1–2), 45–66.

<https://doi.org/10.1080/0035919X.2023.2177361>.

(53) Schneider, L.; Rose, N. L.; Myllyvirta, L.; Haberle, S.; Lintern, A.; Yuan, J.; Sinclair, D.; Holley, C.; Zawadzki, A.; Sun, R. Mercury Atmospheric Emission, Deposition and Isotopic Fingerprinting from Major Coal-Fired Power Plants in Australia: Insights from Palaeo-Environmental Analysis from Sediment Cores. *Environmental Pollution* **2021**, 287, 117596.

<https://doi.org/10.1016/j.envpol.2021.117596>.

(54) Barst, B. D.; Ahad, J. M. E.; Rose, N. L.; Jautzy, J. J.; Drevnick, P. E.; Gammon, P. R.; Sanei, H.; Savard, M. M. Lake-Sediment Record of PAH, Mercury, and Fly-Ash Particle

Deposition near Coal-Fired Power Plants in Central Alberta, Canada. *Environmental Pollution* **2017**, 231, 644–653. <https://doi.org/10.1016/j.envpol.2017.08.033>.

## Appendix 2: Chapter 3 Supplementary information

**Table S.3.1.** The percent weight composition of sediment organic matter, and the bootstrapped concentration of SCPs for each site near the legacy coal fired power plant (sites 1-7) and near the active coal fired power plant (sites 8-14).

Site number	% Organic matter	SCP concentration (SCPs/gDM)
1	0.96	0
2	4.67	7
3	6.14	17
4	5.33	37
5	1.73	2
6	5.51	16
7	1.11	6
8	4.08	45
9	8.18	2138
10	6.41	466
11	2.77	777
12	7.26	169
13	3.80	294
14	2.62	234

**Table S.3.2.** Raw sediment metal concentrations for each element of interest per site. Metal concentrations are in ppm.

Site	Mg	Ca	V	Cr	Fe	Ni	Cu	As	Sr	Mo	Rh	Sb	Tl	Pb
1	4,630.85	3,855.30	18.39	23.00	5,772.20	10.78	42.45	3.99	27.72	4.55	9.95	0.33	0.23	7.36
2	8,152.20	6,441.00	52.26	40.71	13,105.20	19.54	26.65	6.81	100.2	0.93	13.85	0.41	0.36	16.67
3	12,321.20	8,943.70	56.07	43.47	12,119.50	19.65	20.7	3.93	119.56	0.74	11.15	0.38	0.36	16.05
4	5,636.30	4,637.20	68.63	48.61	13,695.40	26.54	25.81	8.05	44.87	1.17	12.42	0.76	0.52	23.89
5	3,749.60	4,084.60	33.75	24.77	6,082.70	10.67	10.37	1.45	51.05	0.39	12.04	0.2	0.2	9.49
6	6,363.70	4,903.60	56.19	39.92	11,823.00	18	20.21	4.97	57.63	0.68	12.76	0.39	0.38	18.6
7	4,280.90	5,914.00	20.66	18.23	5,477.80	8.19	8.75	2.29	15.47	0.28	13.88	0.17	0.15	7.48
8	8,704.60	6,230.10	55.97	39.05	10,449.90	20.49	20.76	6.83	16.53	0.78	12.55	0.49	0.48	23.55
9	7,453.10	6,807.90	66.44	122.43	13,855.40	29.02	33.34	8.46	241.27	1.93	12.21	0.96	0.48	25.59
10	7,691.50	6,585.50	85.19	70.49	17,168.70	31.51	36.26	13.08	10.84	2.03	14.04	1.11	0.72	38.57
11	4,316.30	6,403.20	35.82	25.32	7,022.40	12.79	15.43	4.3	70.93	0.73	12.61	0.46	0.24	12.74
12	7,061.10	10,317.70	79.62	53.88	16,042.90	24.33	27.17	12.76	22.66	1.8	13	0.88	0.5	27.54
13	4,897.70	10,646.30	162.33	44.76	19,778.60	19.04	19.16	21.92	39.19	2.18	12.54	0.77	0.27	91.78
14	4,755.45	10,478.70	88.41	58.59	18,299.20	32.33	38.90	9.43	447.91	3.12	12.91	1.25	0.27	15.36

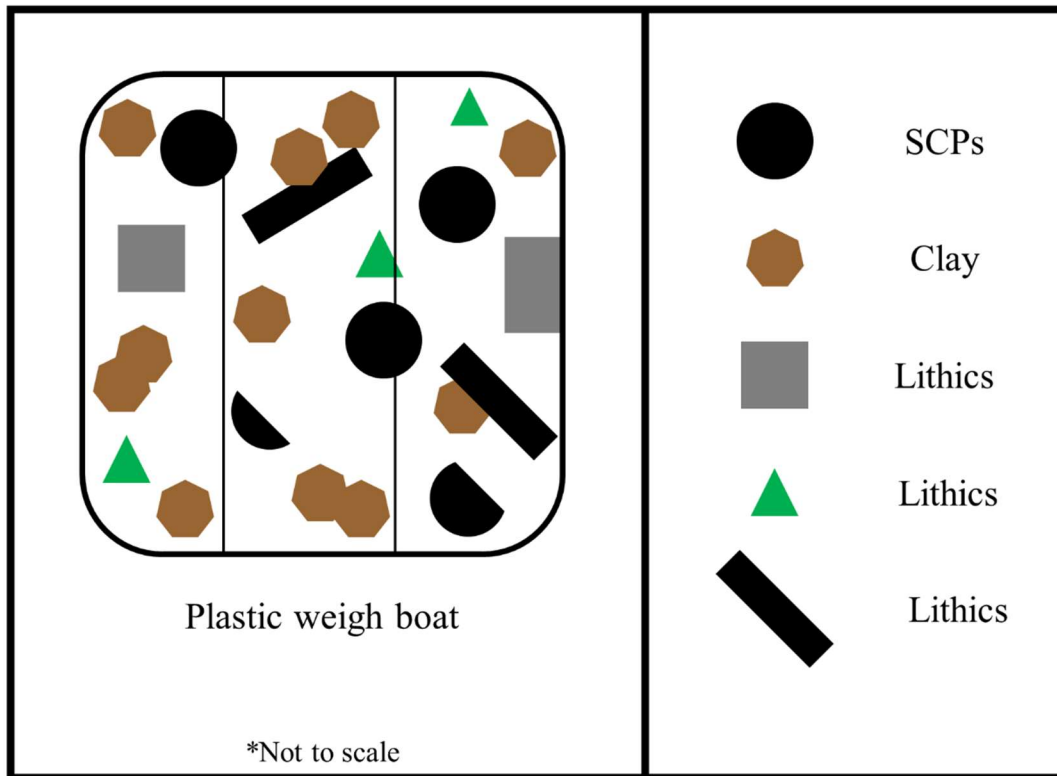


**Figure S.3.1.** Diagram of SCP enumeration strategy under stereomicroscope. Samples were placed in a plastic weigh boat (VWR Catalog No. 76540-490) divided by lines into roughly equal sections. SCPs were enumerated within each section according to criteria from Rose, (1990) in which whole or SCP fragments greater than  $\frac{1}{2}$  of a particle were counted. For particles located on a dividing line, a SCP was counted as within the section that contained greater than  $\frac{1}{2}$  of the particle.